Property-preserving numerical approximations of a Cahn–Hilliard–Navier–Stokes model with variable densities and degenerate mobility

Daniel Acosta-Soba[*][†], Francisco Guillén-González[‡],

J. Rafael Rodríguez-Galván[§], Jin Wang [¶]

April 29, 2024

Abstract

In this paper, we present a new computational framework using coupled and decoupled approximations for a Cahn–Hilliard–Navier–Stokes model with variable densities and degenerate mobility. In this sense, the coupled approximation is shown to conserve the mass of the mixture, preserve the point-wise bounds of the density and decrease an energy functional. In contrast, the decoupled scheme is presented as a more computationally efficient alternative but the discrete energy-decreasing property can not be assured. Both schemes are based on a finite element approximation for the Navier–Stokes fluid flow with discontinuous pressure and an upwind discontinuous Galerkin scheme for the Cahn–Hilliard part. Finally, several numerical experiments contrasting both approaches are conducted. In particular, results for a convergence test, a simple qualitative comparison and some well-known benchmark problems are shown.

Keywords: Mass-conservation. Discrete point-wise bounds. Discrete energy stability. Finite elements. Discontinuous Galerkin. Upwind schemes.

---

[*]Departamento de Matemáticas, Universidad de Cádiz, Puerto Real, 11510 Cádiz, Spain – Email: `daniel.acosta@uca.es` – Corresponding author

[†]Department of Mathematics, University of Tennessee at Chattanooga, Chattanooga, TN 37403, USA

[‡]Departamento de Ecuaciones Diferenciales y Análisis Numérico & IMUS, Universidad de Sevilla, 41012 Seville, Spain – Email: `guillen@us.es`

[§]Departamento de Matemáticas, Universidad de Cádiz, Puerto Real, 11510 Cádiz, Spain – Email: `rafael.rodriguez@uca.es`

[¶]Department of Mathematics, University of Tennessee at Chattanooga, Chattanooga, TN 37403, USA – Email: `jin-wang02@utc.edu`

1   Introduction

Hydrodynamics has been considered a research field of increasing interest among the scientific community during the last few decades. In this sense, diffuse interface models were proposed as a successful alternative to model fluid-solid interaction after van der Waals introduced the foundations in the pioneering paper [42]. Afterwards, these ideas were extended to fluid mixture and several works were published in this regard. In particular, both Hohelberg and Halpering, [29], and Gurtin et al., [28], arrived by different approaches to the same model, the well-known *Model H*, which would lead to the Cahn–Hilliard–Navier–Stokes (CHNS) system.

Since then, many different CHNS models have been developed using different techniques and extended to the case of fluids with different densities, see the model by Boyer [10] or by Ding et al. [19]. Moreover, several of these recent models satisfy some laws of thermodynamics. This is the case for the model by Lowengrub and Truskinovsky, [33], or the one by Abels et al., [1], which introduces an extra convective term in the momentum equation due to the different densities of the fluids. In [30] a careful revision of several CHNS models and their applications is provided. Also, recently, a very interesting survey has been published, [41], in which the authors, Eikelder et al., discuss different existing well-known CHNS models analyzing their advantages and disadvantages from a physical point of view. In fact, the authors of [41] provide some notions on properties a CHNS model has to satisfy in order to be physically consistent.

One characteristic that many of these models share is that the density of the mixture is usually interpolated as a linear function of the phase-field function. Hence, ensuring the point-wise bounds for this phase-field function in the Cahn-Hilliard equation, for instance, by using a degenerate mobility (see [4]) is crucial to ensure a physically consistent model. Also, CHNS models conserve the total mass of the mixture and, as mentioned above, they tend to be thermodynamically consistent in the sense that the solutions of these models usually minimize an underlying energy law. Therefore, as these properties are extremely important for the physical meaning of the models it is likewise important to preserve them when approximating their solutions.

However, the transport of the diffuse interface by the velocity of the fluid is typically modeled by means of a convective term that is introduced into the Cahn-Hilliard equation and, as shown in previous studies such as [4], this term may lead to numerical instabilities in highly convective regimes if it is not treated carefully. The instabilities result in nonphysical spurious oscillations that make the approximation of the phase-field variable lose the point-wise bounds. In this regard, removing the numerical instabilities in the case of the convective Cahn-Hilliard model has been an object of study in several recent works, see [22] or [4], where in the latter the authors enforce the point-wise bounds by means of a discontinuous Galerkin (DG) upwind technique. Different ideas such as the use of limiters have been used in the case of the CHNS systems. For instance, in [31], the authors developed, by means of flux and slope limiters, a bound-preserving decoupled

approximation of a CHNS simplified system with constant mobility. Later, the same model was approximated by high order polynomials using a decoupled scheme and a convex optimization technique with a scaling limiter to ensure the point-wise bounds, see [32].

In addition, designing an approximation that satisfies a discrete version of the continuous energy in the diffuse-interface models is not straightforward and usually requires the use of specific time-discrete approximations such as the standard convex-splitting technique, [21], or the more recently developed SAV approach, [37]. In this sense, several advancements have been made towards the approximation of the CHNS models preserving the energy-stability constraint. For instance, we can find the work [27] where the authors propose an approximation of the model in [1] that decouples the phase-field equations from the fluid equations through a modified velocity. This approach was further studied in [23] and extended to a fully decoupled approximation that uses a pressure correction approach, [38].

Nevertheless, although it has been achieved in the case of a CHNS with a Flory-Huggins logarithmic potential (see [11]), to our best knowledge there is no published work on an approximation of a CHNS model with a Ginzburg-Landau polynomial potential and degenerate mobility that ensures both the mass-conservation, point-wise bounds and energy-stability properties.

To address this challenge, in this work, we provide an upwind DG approximation of the model by Abels et al. [1] where all the mass-conservation, the point-wise bounds and the energy-stability properties are preserved. Moreover, using similar ideas, a decoupled approximation of this model is developed. This decoupled approximation lacks the energy-stability property but is much more computationally efficient than the coupled counterpart.

Firstly, in Section 2 we introduce the CHNS model that we are going to consider and we present its properties. Then, in Section 3 we develop the coupled structure-preserving approximation of the aforementioned model, showing that it satisfies all the mass-conservation, point-wise bounds and energy-stability properties. On the other hand, in Section 4 we introduce the decoupled scheme as a computationally efficient alternative of the coupled counterpart showing that it satisfies both the mass-conservation and the point-wise bounds properties. Finally, in Section 5 we conduct several numerical experiments in which we compare both the coupled and the decoupled approaches. First, we compute a preliminary accuracy test in Subsection 5.1 that suggests that both schemes may have similar convergence order for all the variables in both $L^2(\Omega)$ and $H^1(\Omega)$ norms. Then, we provide a simple test where two bubbles are mixed in Subsection 5.2 to qualitatively compare both approaches. The results are in accordance with the previous theoretical analysis. Also, this test provides an example where the decoupled scheme becomes completely unstable due to the lack of the energy-stability property whereas the coupled counterpart provides a much more trustworthy, energy-decreasing solution. Finally, in Subsections 5.3 and 5.4 we couple the CHNS system with a term modeling the action of gravitational forces and conduct two benchmark tests: a heavier bubble in a lighter medium and a Rayleigh-Taylor type instability.

2 Cahn–Hilliard–Navier–Stokes model

Let $\Omega \subset \mathbb{R}^d$ be a bounded polygonal domain. We consider a mixture of two fluids with different densities $0 < \rho_1 < \rho_2$ and introduce a phase-field function $\phi = \phi(t, x) \in [-1, 1]$ such that $\phi = -1$ corresponds with fluid of density ρ_1, $\phi = 1$ with fluid of density ρ_2 and $\phi \in (-1, 1)$ in the interface between the two fluids. Then, the diffuse-interface Cahn–Hilliard–Navier–Stokes model proposed by Abels et al. in [1] and further numerically studied in [23, 27, 38], can be written as follows:

$$\rho(\phi)\mathbf{u}_t + ((\rho(\phi)\mathbf{u} - \mathbf{J}) \cdot \nabla)\mathbf{u} - \nabla \cdot (2\eta(\phi)\mathbf{Du}) + \nabla p + \phi\nabla\mu = 0 \quad \text{in } \Omega \times (0, T), \tag{1a}$$

$$\nabla \cdot \mathbf{u} = 0 \quad \text{in } \Omega \times (0, T), \tag{1b}$$

$$\phi_t + \nabla \cdot (\phi\mathbf{u}) - \nabla \cdot (M(\phi)\nabla\mu) = 0 \quad \text{in } \Omega \times (0, T), \tag{1c}$$

$$-\lambda\varepsilon\Delta\phi + \frac{\lambda}{\varepsilon}f(\phi) = \mu \quad \text{in } \Omega \times (0, T), \tag{1d}$$

$$\mathbf{u}(0) = \mathbf{u}_0, \quad \phi(0) = \phi_0 \quad \text{in } \Omega, \tag{1e}$$

$$\mathbf{u} = 0, \quad \nabla\phi \cdot \mathbf{n} = 0, \quad M(\phi)\nabla\mu \cdot \mathbf{n} = 0 \quad \text{on } \partial\Omega. \tag{1f}$$

Here, $\mathbf{u}$ and p are the mean velocity and the pressure of the fluid respectively, and μ is the chemical potential related to the phase-field function ϕ. Also, $\mathbf{Du} = \frac{1}{2}(\nabla\mathbf{u} + \nabla\mathbf{u}^t)$ is the strain tensor, $f(\phi)$ is the derivative of the Ginzburg-Landau double well potential $F(\phi) = \frac{1}{4}(\phi^2 - 1)^2$, i.e. $f(\phi) = F'(\phi) = (\phi^2 - 1)\phi$, $M(\phi) = (1 - \phi^2)_\oplus$ is the degenerate (truncated) mobility function and

$$\mathbf{J} = \frac{\rho_2 - \rho_1}{2}M(\phi)\nabla\mu$$

is the extra-convective term due to different densities. Moreover, the density of the mixture $\rho = \rho(\phi)$ depending on the phase-field variable ϕ, can be defined either as the solution of the mass balance equation

$$(\partial_t\rho, \overline{\rho}) - (\rho\mathbf{u} - \mathbf{J}, \nabla\overline{\rho}) = 0, \quad \forall\overline{\rho} \in H^1(\Omega), \quad \text{in } (0, T), \tag{2}$$

or, by taking into account the equation (1c), as the explicit relation

$$\rho(\phi) = \frac{\rho_1 + \rho_2}{2} + \frac{\rho_2 - \rho_1}{2}\phi := \rho_{\text{avg}} + \rho_{\text{dif}}\phi. \tag{3}$$

Remark 2.1. *We have written the equation* (2) *in its more general variational formulation since* $\mathbf{J}$ *does not necessarily belong to* $H^1(\Omega)^d$. *It is clear from* (3) *that* $\rho_1 \leq \rho(\phi) \leq \rho_2$ *in* $\Omega \times (0, T)$ *is equivalent to* $-1 \leq \phi \leq 1$ *in* $\Omega \times (0, T)$. *Consequently, it is important the constraint* $\phi \in [-1, 1]$ *to preserve the physical meaning of the model because the density of the mixture* $\rho(\phi)$ *must satisfy* $\rho(\phi) \in [\rho_1, \rho_2]$.

Finally, $\eta \in \mathcal{C}([-1, 1])$ with $\eta(\phi) \geq C$ for certain $C > 0$ and for all $\phi \in [-1, 1]$ is the viscosity of the mixture, $\lambda > 0$ is a constant related to the energy density and $\varepsilon > 0$ is a small parameter related to the thickness of the interface between the two fluids.

Since if p is a pressure function solution of (1) then $p + C$ is also solution for any constant C, it is usual to consider the zero mean-value pressure constraint $\int_\Omega p = 0$.

We can consider the following variational formulation of problem (1): Find $(\mathbf{u}, p, \phi, \mu)$ such that $\mathbf{u} \in L^\infty(0, T; L^2(\Omega)^d) \cap L^2(0, T; H_0^1(\Omega)^d)$, $p \in W^{-1,\infty}(0, T; L^2(\Omega))$ with $\int_\Omega p = 0$, $\phi \in L^\infty(0, T; H^1(\Omega))$ with $-1 \leq \phi \leq 1$ a.e. in $\Omega \times (0, T)$, $\mu : \Omega \times (0, T) \to \mathbb{R}$ with $\sqrt{M(\phi)}\nabla\mu \in L^2(0, T; L^2(\Omega))$, satisfying

$$\langle \rho(\phi)\mathbf{u}_t, \overline{\mathbf{u}}\rangle + ([(\rho(\phi)\mathbf{u} - \rho_{\text{dif}}M(\phi)\nabla\mu) \cdot \nabla]\,\mathbf{u}, \overline{\mathbf{u}})$$
$$+2\,(\eta(\phi)\mathbf{Du}, \mathbf{D\overline{u}}) - (p, \nabla \cdot \overline{\mathbf{u}}) - (\mu, \nabla \cdot (\phi\overline{\mathbf{u}})) = 0, \tag{4a}$$

$$(\nabla \cdot \mathbf{u}, \overline{p}) = 0, \tag{4b}$$

$$\langle \phi_t, \overline{\phi}\rangle + (\nabla \cdot (\phi\mathbf{u}), \overline{\phi}) + (M(\phi)\nabla\mu, \nabla\overline{\phi}) = 0, \tag{4c}$$

$$\lambda\varepsilon\,(\nabla\phi, \nabla\overline{\mu}) + \frac{\lambda}{\varepsilon}\,(f(\phi), \overline{\mu}) - (\mu, \overline{\mu}) = 0, \tag{4d}$$

for each $(\overline{\mathbf{u}}, \overline{p}, \overline{\mu}, \overline{\phi}) \in (H_0^1(\Omega) \cap L^\infty(\Omega))^d \times L^2(\Omega) \times H^1(\Omega) \times H^1(\Omega)$. We have denoted $(f, g) = \int_\Omega f\,g$ as the $L^2(\Omega)$ scalar product and

$$(\eta(\phi)\mathbf{Du}, \mathbf{D\overline{u}}) = \int_\Omega \eta(\phi)\mathbf{Du} : \mathbf{D\overline{u}},$$

where : denotes the Frobenius inner product.

Proposition 2.2. *The mass of the phase-field variable is conserved, because it holds*

$$\frac{d}{dt}\int_\Omega \phi(t, x)dx = 0.$$

In particular, the mass of the mixture is conserved, because using (3),

$$\int_\Omega \rho(\phi(t, x))dx = |\Omega|\rho_{avg} + \rho_{dif}\int_\Omega \phi(t, x)dx = |\Omega|\rho_{avg} + \rho_{dif}\int_\Omega \phi_0(x)dx = \int_\Omega \rho(\phi_0(x))dx.$$

Proof. Just test (4c) by $\overline{\phi} = 1$. $\qquad\qquad\qquad\qquad\qquad\qquad\qquad\qquad\qquad\qquad\qquad\qquad\qquad$ □

Proposition 2.3. *Assuming a sufficiently regular solution of* (4a)-(4d), *the following energy law holds:*

$$\frac{d}{dt}E(\mathbf{u}, \phi) + 2\int_\Omega \eta(\phi)|\mathbf{Du}|^2 + \int_\Omega M(\phi)|\nabla\mu|^2 = 0, \tag{5}$$

where $|\mathbf{Du}|^2 = \sum_{i=1}^d |\mathbf{Du}_i|^2$, *with* $\mathbf{Du}_i$ *denoting the* i-*th row of the stress tensor* $\mathbf{Du}$, *and*

$$E(\mathbf{u}, \phi) := \int_\Omega \rho(\phi)\frac{|\mathbf{u}|^2}{2} + \frac{\lambda\varepsilon}{2}\int_\Omega |\nabla\phi|^2 + \frac{\lambda}{\varepsilon}\int_\Omega F(\phi), \tag{6}$$

where the first term is associated to the kinetic energy and the others to the potential energy. In particular, the energy $E(\mathbf{u}, \phi)$ *is time decreasing because*

$$\frac{d}{dt}E(\mathbf{u}, \phi) \leq 0.$$

Proof. We argue formally, by considering that all the functions that appear below are regular enough so that the expressions are true. Moreover, they are regarded as functions to be evaluated at $t \in (0, T)$, although, for clarity, we will omit it.

If we test (4a)–(4d) by $\overline{\mathbf{u}} = \mathbf{u}$, $\overline{p} = p$, $\overline{\phi} = \mu$ and $\overline{\mu} = \phi_t$ and we add up the expressions, we obtain:

$$
(\rho(\phi)\mathbf{u}_t, \mathbf{u}) + \lambda\varepsilon\left(\nabla\phi, \nabla\phi_t\right) + \frac{\lambda}{\varepsilon}\left(F'(\phi), \phi_t\right)
$$
$$
+ \left([(\rho(\phi)\mathbf{u} - \mathbf{J}) \cdot \nabla]\,\mathbf{u}, \mathbf{u}\right) + 2\int_\Omega \eta(\phi)|\mathbf{Du}|^2 + \int_\Omega M(\phi)|\nabla\mu|^2 = 0.
$$

Now, testing (2) by $\overline{\rho} = |\mathbf{u}|^2/2$, we have

$$
\left(\partial_t\rho(\phi), \frac{|\mathbf{u}|^2}{2}\right) - \left([(\rho(\phi)\mathbf{u} - \mathbf{J}) \cdot \nabla]\mathbf{u}, \mathbf{u}\right) = 0.
$$

By adding the two previous expressions, the convective term $\left([(\rho(\phi)\mathbf{u} - \mathbf{J}) \cdot \nabla]\mathbf{u}, \mathbf{u}\right)$ cancels. Hence, taking into account that

$$
\frac{d}{dt}\int_\Omega \rho(\phi)\frac{|\mathbf{u}|^2}{2} = (\rho(\phi)\mathbf{u}_t, \mathbf{u}) + \left(\partial_t\rho(\phi), \frac{|\mathbf{u}|^2}{2}\right),
$$
$$
\frac{1}{2}\frac{d}{dt}\int_\Omega |\nabla\phi|^2 = (\nabla\phi, \nabla\phi_t),
$$
$$
\frac{d}{dt}\int_\Omega F(\phi) = (F'(\phi), \phi_t),
$$

we can conclude that the energy law (5) holds. □

3 Coupled structure-preserving scheme

In this section we develop a fully coupled discretization of the model (1) that preserves all properties at the discrete level, including the mass conservation, point-wise bounds of the phase-field and density of the mixture variables, and the decreasing of the energy (also called energy-stability).

3.1 Notation

We consider a finite element shape-regular triangular mesh $\mathcal{T}_h = \{K\}_{K\in\mathcal{T}_h}$ in the sense of Ciarlet, [14], of size h over Ω. We denote by $\mathcal{E}_h$ the set of the edges of $\mathcal{T}_h$ (faces if $d = 3$) with $\mathcal{E}_h^{\mathrm{i}}$ the set of the *interior edges* and $\mathcal{E}_h^{\mathrm{b}}$ the *boundary edges*, i.e. $\mathcal{E}_h = \mathcal{E}_h^{\mathrm{i}} \cup \mathcal{E}_h^{\mathrm{b}}$.

Now, we fix the following orientation over the mesh $\mathcal{T}_h$:

- For any interior edge $e \in \mathcal{E}_h^{\mathrm{i}}$ we set the associated unit normal vector $\mathbf{n}_e$. In this sense, when refering to edge $e \in \mathcal{E}_h^{\mathrm{i}}$ we will denote by K_e and L_e the elements of $\mathcal{T}_h$ with $e = \partial K_e \cap \partial L_e$ and so that $\mathbf{n}_e$ is exterior to K_e pointing to L_e.

If there is no ambiguity, to abbreviate the notation we will denote the previous elements K_e and L_e simply by K and L, respectively, with the assumption that their naming is always with respect to the edge $e \in \mathcal{E}_h^i$ and it may vary if we consider a different edge of $\mathcal{E}_h^i$.

- For any boundary edge $e \in \mathcal{E}_h^b$, the unit normal vector $\mathbf{n}_e$ points outwards of the domain Ω.

Therefore, we can define the *average* $\{\!\{\cdot\}\!\}$ and the *jump* $[\![\cdot]\!]$ of a function v on an edge $e \in \mathcal{E}_h$ as follows:

$$\{\!\{v\}\!\} := \begin{cases} \dfrac{v_K + v_L}{2} & \text{if } e \in \mathcal{E}_h^i, \ e = K \cap L, \\ v_K & \text{if } e \in \mathcal{E}_h^b, \ e \subset K, \end{cases} \qquad [\![v]\!] := \begin{cases} v_K - v_L & \text{if } e \in \mathcal{E}_h^i, \ e = K \cap L, \\ v_K & \text{if } e \in \mathcal{E}_h^b, \ e \subset K. \end{cases}$$

We denote by $\mathbb{P}_k^{\mathrm{disc}}(\mathcal{T}_h)$ and $\mathbb{P}_k^{\mathrm{cont}}(\mathcal{T}_h)$ the spaces of finite element discontinuous and continuous functions, respectively, which are polynomials of degree $k \geq 0$ when restricted to the elements K of $\mathcal{T}_h$. In this sense, we will denote the broken differential operators (see [17, 34]) the same way than the standard differential operators in the absence of ambiguity.

Moreover, we take an equispaced partition $0 = t_0 < t_1 < \cdots < t_N = T$ of the time domain $[0, T]$ with $\Delta t = t_{m+1} - t_m$ the time step. Also, for any function v depending on time, we denote $v^{m+1} \simeq v(t_{m+1})$ and the discrete time derivative operator $v_t(t_{m+1}) \simeq \delta_t v^{m+1} := (v^{m+1} - v^m)/\Delta t$.

Finally, we set the following notation for the positive and negative parts of a function v:

$$v_\oplus := \frac{|v| + v}{2} = \max\{v, 0\}, \quad v_\ominus := \frac{|v| - v}{2} = -\min\{v, 0\}, \quad v = v_\oplus - v_\ominus.$$

3.2 Discrete scheme

Following the ideas of [2, 3, 4] we define the projections $\Pi_0 \colon L^1(\Omega) \longrightarrow \mathbb{P}_0^{\mathrm{disc}}(\mathcal{T}_h)$, $\Pi_1 \colon L^1(\Omega) \longrightarrow \mathbb{P}_1^{\mathrm{cont}}(\mathcal{T}_h)$ and $\Pi_1^h \colon L^1(\Omega) \longrightarrow \mathbb{P}_1^{\mathrm{cont}}(\mathcal{T}_h)$ as follows:

$$(\Pi_0 g, \overline{w}) = (g, \overline{w}), \qquad\qquad \forall \overline{w} \in \mathbb{P}_0^{\mathrm{disc}}(\mathcal{T}_h) \tag{7}$$

$$(\Pi_1 g, \overline{v}) = (g, \overline{v}), \qquad\qquad \forall \overline{v} \in \mathbb{P}_1^{\mathrm{cont}}(\mathcal{T}_h), \tag{8}$$

$$\left(\Pi_1^h g, \overline{v}\right)_h = (g, \overline{v}), \qquad\qquad \forall \overline{v} \in \mathbb{P}_1^{\mathrm{cont}}(\mathcal{T}_h), \tag{9}$$

where $(\cdot, \cdot)$ and $(\cdot, \cdot)_h$ denote the usual scalar product in $L^2(\Omega)$ and the mass-lumping scalar product in $\mathbb{P}_1^{\mathrm{cont}}(\mathcal{T}_h)$, respectively.

We propose the following numerical scheme: find $\mathbf{u}^{m+1} \in \mathcal{U}_h$, $p^{m+1} \in \mathcal{P}_h$ with $\int_\Omega p^{m+1} = 0$,

$\phi^{m+1} \in \mathbb{P}_0^{\text{disc}}(\mathcal{T}_h)$ and $\mu^{m+1} \in \mathbb{P}_1^{\text{cont}}(\mathcal{T}_h)$ such that

$$
\begin{aligned}
&\left(\rho(\Pi_1^h\phi^m)\delta_t\mathbf{u}^{m+1}, \overline{\mathbf{u}}\right) + \left(\left[\left(\rho(\Pi_1^h\phi^m)u^m - \mathbf{J}_h^m\right)\cdot\nabla\right]\mathbf{u}^{m+1}, \overline{\mathbf{u}}\right) \\
&+2\left(\eta(\phi^m)\mathbf{D}\mathbf{u}^{m+1}, \mathbf{D}\overline{\mathbf{u}}\right) - \left(p^{m+1}, \nabla\cdot\overline{\mathbf{u}}\right) + c_h(\phi^{m+1}, \Pi_0\mu^{m+1}, \overline{\mathbf{u}}) \\
&+s_h^1(\mathbf{u}^{m+1}, \mathbf{u}^m, \Pi_1^h\phi^{m+1}, \Pi_1^h\phi^m, \mu^m, \overline{\mathbf{u}}) + s_h^2(\mathbf{u}^{m+1}, \phi^{m+1}, \Pi_0\mu^{m+1}, \overline{\mathbf{u}}) = 0, &&\text{(10a)}
\end{aligned}
$$

$$
\left(\nabla\cdot\mathbf{u}^{m+1}, \overline{p}\right) = 0, \qquad\qquad\text{(10b)}
$$

$$
\left(\delta_t\phi^{m+1}, \overline{\phi}\right) + a_h^{\text{upw}}(\mathbf{u}^{m+1}; \phi^{m+1}, \overline{\phi}) + b_h^{\text{upw}}(\nabla_\mathbf{n}^0\mu^{m+1}; M(\phi^{m+1}), \overline{\phi}) = 0, \qquad\text{(10c)}
$$

$$
\lambda\varepsilon\left(\nabla(\Pi_1^h\phi^{m+1}), \nabla\overline{\mu}\right) + \frac{\lambda}{\varepsilon}\left(f(\Pi_1^h\phi^{m+1}, \Pi_1^h\phi^m), \overline{\mu}\right) - \left(\mu^{m+1}, \overline{\mu}\right)_h = 0, \qquad\text{(10d)}
$$

for each $\overline{\mathbf{u}} \in \mathcal{U}_h$, $\overline{p} \in \mathcal{P}_h$, $\overline{\phi} \in \mathbb{P}_0^{\text{disc}}(\mathcal{T}_h)$, $\overline{\mu} \in \mathbb{P}_1^{\text{cont}}(\mathcal{T}_h)$, where

$$
\mathbf{J}_h^m = \rho_{\text{dif}}M(\Pi_1^h\phi^m)\Pi_1(\nabla\mu^m),
$$

and

$$
f(\phi_1, \phi_0) := F_i'(\phi_1) + F_e'(\phi_0) \text{ with } F_i(\phi) := \phi^2 + \frac{1}{4}, \ F_e(\phi) := \frac{1}{4}\phi^4 - \frac{3}{2}\phi^2 \qquad\text{(11)}
$$

such that $F(\phi) = F_i(\phi) + F_e(\phi)$ is a convex splitting discretization of the Ginzburg-Landau double well potential $F(\phi)$ for any $\phi \in [-1, 1]$.

Also, $(\mathcal{U}_h, \mathcal{P}_h)$ is a compatible "inf-sup" pair of finite-dimensional spaces satisfying that $\mathcal{U}_h \subset (\mathcal{C}^0(\overline{\Omega}) \cap H_0^1(\Omega))^d$ and $\mathbb{P}_0^{\text{disc}}(\mathcal{T}_h) \subset \mathcal{P}_h$. In fact, the restriction $\mathbb{P}_0^{\text{disc}}(\mathcal{T}_h) \subset \mathcal{P}_h$ is needed in order to guarantee the local incompressibility of $\mathbf{u}^{m+1}$ in the following sense:

$$
\sum_{e\in\mathcal{E}_h^i}\int_e(\mathbf{u}^{m+1}\cdot\mathbf{n}_e)[\![\overline{p}]\!] = 0, \quad \forall\overline{p} \in \mathbb{P}_0^{\text{disc}}(\mathcal{T}_h), \qquad\text{(12)}
$$

which can be derived integrating by parts in (10b). This constraint will allow us to preserve the point-wise bounds of ϕ^{m+1}, see Theorem 3.5 below. Notice that the discretization of the pressure and the divergence term (10b) is the standard Stokes DG approach [17, 34] for continuous velocity and discontinuous pressure.

Remark 3.1. *Some possible choices of compatible spaces $(\mathcal{U}_h, \mathcal{P}_h)$ are the following (see [9, 20] for the details):*

- *$(\mathcal{U}_h, \mathcal{P}_h) = ((\mathbb{P}_2^{cont}(\mathcal{T}_h) \cap H_0^1(\Omega))^d, \mathbb{P}_0^{disc}(\mathcal{T}_h))$ which is stable for $d = 2$ but not for $d = 3$.*

- *$(\mathcal{U}_h, \mathcal{P}_h) = ((\mathbb{P}_2^{bubble}(\mathcal{T}_h) \cap H_0^1(\Omega))^d, \mathbb{P}_1^{disc}(\mathcal{T}_h))$ which is stable for $d = 2, 3$ but requires a higher computational effort. Here, $\mathbb{P}_2^{bubble}(\mathcal{T}_h)$ denotes the $\mathbb{P}_2^{cont}(\mathcal{T}_h)$ space enriched with a bubble by elements of order 3.*

Notice that, for any choice of this pair $(\mathcal{U}_h, \mathcal{P}_h)$, the error bounds are expected to be determined by the lowest accuracy approximation of the phase-field function by $\mathbb{P}_0^{\text{disc}}(\mathcal{T}_h)$.

Moreover, $c_h(\phi, \mu, \overline{\mathbf{u}})$ is a centered discretization of the term $(\phi \nabla \mu, \overline{\mathbf{u}}) = -(\mu, \nabla \cdot (\phi \overline{\mathbf{u}}))$ in (4a) defined as

$$c_h(\phi, \mu, \overline{\mathbf{u}}) := -\int_\Omega \nabla \cdot (\phi \overline{\mathbf{u}}) \mu - \sum_{e \in \mathcal{E}_h^i} \int_e (\overline{\mathbf{u}} \cdot \mathbf{n}_e) \{\!\{\phi\}\!\} [\![\mu]\!], \tag{13}$$

where the second term is a consistent stabilization term depending on the jumps of μ on the interior edges of the mesh $\mathcal{T}_h$.

In (10c) we have considered two different upwind formulas, the classical upwind

$$a_h^{\mathrm{upw}}(\mathbf{u}; \phi, \overline{\phi}) := \sum_{e \in \mathcal{E}_h^i, e = K \cap L} \int_e ((\mathbf{u} \cdot \mathbf{n}_e)_\oplus \phi_K - (\mathbf{u} \cdot \mathbf{n}_e)_\ominus \phi_L) [\![\phi]\!] \tag{14}$$

whose properties were discussed in [4], and

$$b_h^{\mathrm{upw}}(\nabla_{\mathbf{n}}^0 \mu; M(\phi), \overline{\phi}),$$

which follows the ideas introduced in [2, 3], and which will be detailed in the Subsection 3.2.1.

Finally, we have introduced in (10a) two consistent stabilizations terms:

$$s_h^1(\mathbf{u}_1, \mathbf{u}_0, \phi_1, \phi_0, \mu, \overline{\mathbf{u}}) := \frac{1}{2} \Big\{ (\delta_t \rho(\phi_1), \mathbf{u}_1 \cdot \overline{\mathbf{u}}) - (\rho(\phi_0) \mathbf{u}_0 - \rho_{\mathrm{dif}} M(\phi_0) \Pi_1(\nabla \mu), \nabla(\mathbf{u}_1 \cdot \overline{\mathbf{u}})) \Big\}, \tag{15}$$

which, following the ideas of [27], can be interpreted as a residual to the equation (2); and

$$s_h^2(\mathbf{u}, \phi, \mu, \overline{\mathbf{u}}) := -\frac{1}{2} \sum_{e \in \mathcal{E}_h^i} \int_e (\overline{\mathbf{u}} \cdot \mathbf{n}_e) \operatorname{sign}(\mathbf{u} \cdot \mathbf{n}_e) [\![\phi]\!] [\![\mu]\!], \tag{16}$$

which is introduced to control the influence of the upwind term $a_h^{\mathrm{upw}}(\mathbf{u}^{m+1}; \phi^{m+1}, \overline{\phi})$ in (10c). This latter stabilization together with the centered approximation $c_h(\phi^{m+1}, \Pi_0 \mu^{m+1}, \overline{\mathbf{u}})$ of the phase-field force in the momentum equation (10a), cancel the effect of the transport of the phase-field function by the mean velocity $\mathbf{u}^{m+1}$ and allow us to obtain a discrete energy inequality, see Lemma 3.7 below.

To start the algorithm we take $\phi^0 = \Pi_0 \phi_0$ where ϕ_0 is the continuous initial data, which satisfies $\phi_0 \in [-1, 1]$. Notice that, one also has $\phi^0 \in [-1, 1]$.

Remark 3.2. *Observe that the 0-mean value constraint on the pressure has been removed from the discrete formulation (10). This constraint will be enforced in practice by using an additional penalty term, see Section 5 below.*

3.2.1 Definition of the upwind bilinear form $b_h^{\mathrm{upw}}(\cdot; \cdot, \cdot)$

In order to define the upwind bilinear form $b_h^{\mathrm{upw}}(\cdot; \cdot, \cdot)$ we follow the ideas of [2, 3].

First, we split the mobility function $M(z)$ for $z \in \mathbb{R}$ into its increasing and decreasing parts, denoted respectively by $M^\uparrow(z)$ and $M^\downarrow(z)$, as follows:

$$M^\uparrow(z) = \int_{-1}^{\min(z,1)} M'(s)_\oplus ds = \int_{-1}^{\min(z,1)} (-2s)_\oplus ds,$$

$$M^\downarrow(z) = -\int_{-1}^{\min(z,1)} M'(s)_\ominus ds = -\int_{-1}^{\min(z,1)} (-2s)_\ominus ds$$

Therefore,

$$M^\uparrow(z) = \begin{cases} M(z) & \text{if } z \le 0 \\ M(0) & \text{if } z > 0 \end{cases}, \quad M^\downarrow(z) = \begin{cases} 0 & \text{if } z \le 0 \\ M(z) - M(0) & \text{if } z > 0 \end{cases}. \tag{18}$$

Notice that $M^\uparrow(z) + M^\downarrow(z) = M(z)$.

Following the work in [4], we can define the following upwind form for any $\phi, \overline{\phi} \in \mathbb{P}_0^{\text{disc}}(\mathcal{T}_h)$ and $\mu \in \mathbb{P}_1^{\text{cont}}(\mathcal{T}_h)$:

$$b_h^{\text{upw}}(-\nabla_{\mathbf{n}}\mu; M(\phi), \overline{\phi}) :=$$
$$\sum_{e \in \mathcal{E}_h^{\text{i}}, e = K \cap L} \int_e \left((-\nabla_{\mathbf{n}}\mu)_\oplus (M^\uparrow(\phi_K) + M^\downarrow(\phi_L))_\oplus - (-\nabla_{\mathbf{n}}\mu)_\ominus (M^\uparrow(\phi_L) + M^\downarrow(\phi_K))_\oplus \right) [\![\overline{\phi}]\!], \tag{19}$$

where $\nabla_{\mathbf{n}}\mu := \{\!\{\nabla\mu\}\!\} \cdot \mathbf{n}_e$ on every $e \in \mathcal{E}_h$.

Nonetheless, if we want to ensure a discrete energy law, as was done in [2, 3], we need to introduce the following hypothesis:

Hypothesis 1. The mesh $\mathcal{T}_h$ of $\overline{\Omega}$ is structured in the sense that, for any interior interface $e = K \cap L \in \mathcal{E}_h^{\text{i}}$, the line between the barycenters of K and L is orthogonal to e.

Under this hypothesis, we can consider the following consistent approximation on every $e \in \mathcal{E}_h^i$, as done in [2, 3]:

$$\nabla\mu \cdot \mathbf{n}_e \simeq \frac{-[\![\Pi_0\mu]\!]}{\mathcal{D}_e(\mathcal{T}_h)} := \nabla_{\mathbf{n}}^0\mu|_e, \tag{20}$$

where $\mathcal{D}_e(\mathcal{T}_h)$ is the distance between the barycenters of the triangles of the mesh $\mathcal{T}_h$ that share $e \in \mathcal{E}_h^i$.

Therefore, we can extend the definition of the upwind bilinear form (19) as follows:

$$b_h^{\text{upw}}(-\nabla_{\mathbf{n}}^0\mu; M(\phi), \overline{\phi})$$
$$= \sum_{e \in \mathcal{E}_h^{\text{i}}, e = K \cap L} \frac{1}{\mathcal{D}_e(\mathcal{T}_h)} \int_e \left(([\![\Pi_0\mu]\!])_\oplus (M^\uparrow(\phi_K) + M^\downarrow(\phi_L))_\oplus - ([\![\Pi_0\mu]\!])_\ominus (M^\uparrow(\phi_L) + M^\downarrow(\phi_K))_\oplus \right) [\![\overline{\phi}]\!]. \tag{21}$$

This upwind approximation allows us to obtain both a discrete maximum principle and an energy-stability property as shown in [2] for a tumor model based on the Cahn-Hilliard equation with degenerate mobility.

Remark 3.3. *Notice that the upwind bilinear form $a_h^{upw}(\mathbf{u}; \phi, \overline{\phi})$ given in (14), can be seen as a particular case of $b_h^{upw}(\cdot; \cdot, \cdot)$ given in (19), changing $M(\phi)$ by ϕ, but now we have not truncated the transported variable ϕ. In fact, it is not necessary to truncate ϕ in $a_h^{upw}(\mathbf{u}; \phi, \overline{\phi})$ to preserve the point-wise bounds of ϕ due to the local incompressibility of $\mathbf{u}$ (see [4] for a more detailed explanation).*

3.2.2 Properties of the scheme (10)

Proposition 3.4 (Mass conservation)**.** *The mass of the phase-field variable and its regularization are conserved. In fact, one has*

$$\int_\Omega \phi^{m+1} = \int_\Omega \phi^m, \quad \int_\Omega \Pi_1^h \phi^{m+1} = \int_\Omega \Pi_1^h \phi^m.$$

As a consequence, since $\rho(\phi)$ is linear with respect to ϕ, the mass of the mixture is also conserved,

$$\int_\Omega \rho(\phi^{m+1}) = \int_\Omega \rho(\phi^m), \quad \int_\Omega \rho(\Pi_1^h \phi^{m+1}) = \int_\Omega \rho(\Pi_1^h \phi^m).$$

Proof. Just need to take $\overline{\phi} = 1$ in (10c) and consider the definitions of the regularization Π_1^h given in (9), and the density of the mixture $\rho(\phi)$ given in (3). $\qquad\square$

Theorem 3.5 (Point-wise bounds of the phase-field variable)**.** *Provided that $\phi^m \in [-1, 1]$ in Ω, any solution ϕ^{m+1} of (10) and $\Pi_1^h \phi^{m+1}$ satisfy: $\phi^{m+1}, \Pi_1^h \phi^{m+1} \in [-1, 1]$ in Ω.*

Proof. To prove that $\phi^{m+1} \geq -1$ in Ω we may take the following $\mathbb{P}_0^{\mathrm{disc}}(\mathcal{T}_h)$ test function

$$\overline{\phi}^* = \begin{cases} (\phi_{K^*}^{m+1} + 1)_\ominus & \text{in } K^* \\ 0 & \text{out of } K^* \end{cases},$$

where K^* is an element of $\mathcal{T}_h$ such that $\phi_{K^*}^{m+1} = \min_{K \in \mathcal{T}_h} \phi_K^{m+1}$. We denote $\mathbf{n}_{K^*}$ the normal vector exterior to K^*. Then, since $\phi_L^{m+1} \geq \phi_{K^*}^{m+1}$ we can assure, using the local incompressibility constraint (12), that

$$a_h^{upw}(\mathbf{u}^{m+1}; \phi^{m+1}, \overline{\phi}^*) = \sum_{e \in \mathcal{E}_h^i} \int_e \left((\mathbf{u}^{m+1} \cdot \mathbf{n}_e)_\oplus \phi_K^{m+1} - (\mathbf{u}^{m+1} \cdot \mathbf{n}_e)_\ominus \phi_L^{m+1} \right) \left[\!\left[\overline{\phi}^* \right]\!\right]$$

$$= \sum_{e \in \mathcal{E}_h^i, e = K^* \cap L} \int_e \left((\mathbf{u}^{m+1} \cdot \mathbf{n}_{K^*})_\oplus \phi_{K^*}^{m+1} - (\mathbf{u}^{m+1} \cdot \mathbf{n}_{K^*})_\ominus \phi_L^{m+1} \right) (\phi_{K^*}^{m+1} + 1)_\ominus$$

$$\leq \sum_{e \in \mathcal{E}_h^i, e \subset K^*} \int_e (\mathbf{u}^{m+1} \cdot \mathbf{n}_{K^*}) \phi_{K^*}^{m+1} (\phi_{K^*}^{m+1} + 1)_\ominus$$

$$= \sum_{e \in \mathcal{E}_h^i} \int_e (\mathbf{u}^{m+1} \cdot \mathbf{n}_e) \left[\!\left[\phi^{m+1} \overline{\phi}^* \right]\!\right] = 0.$$

11

On the other hand, using that the positive part is an increasing function and that

$$M^{\uparrow}(\phi_L^{m+1}) \geq M^{\uparrow}(\phi_{K^*}^{m+1}) \quad \text{and} \quad M^{\downarrow}(\phi_L^{m+1}) \leq M^{\downarrow}(\phi_{K^*}^{m+1}),$$

we can obtain (see [2, 4])

$$b_h^{\text{upw}}(\nabla_{\mathbf{n}}^0 \mu^{m+1}; M(\phi^{m+1}), \overline{\phi}^*) \leq 0.$$

Consequently, $|K^*| \delta_t u_{K^*}^{m+1}(u_{K^*}^{m+1} + 1)_{\ominus} \geq 0$. Therefore,

$$0 \leq |K^*|(\delta_t(\phi_{K^*}^{m+1} + 1))(\phi_{K^*}^{m+1} + 1)_{\ominus} = -\frac{|K^*|}{\Delta t}\left((\phi_{K^*}^{m+1} + 1)_{\ominus}^2 + (\phi_{K^*}^m + 1)(\phi_{K^*}^{m+1} + 1)_{\ominus}\right) \leq 0,$$

which implies, since $\phi_{K^*}^m \geq -1$, that $(\phi_{K^*}^{m+1} + 1)_{\ominus} = 0$. Hence, $\phi^{m+1} \geq -1$ in Ω.

Similarly, taking the following $\mathbb{P}_0^{\text{disc}}(\mathcal{T}_h)$ test function

$$\overline{\phi}^* = \begin{cases} (\phi_{K^*}^{m+1} - 1)_{\oplus} & \text{in } K^* \\ 0 & \text{out of } K^* \end{cases},$$

where K^* is an element of $\mathcal{T}_h$ such that $\phi_{K^*}^{m+1} = \max_{K \in \mathcal{T}_h} \phi_K^{m+1}$, we can arrive at $\phi^{m+1} \leq 1$ in Ω.

Finally, $\Pi_1^h \phi^{m+1} \in [-1, 1]$ in Ω is a direct consequence of the definition of the projection Π_1^h given in (9). □

The next Corollary is a direct consequence of the previous result.

Corollary 3.6 (Point-wise bounds of the mixture density). *Provided that $\rho(\phi^m) \in [\rho_1, \rho_2]$ in Ω, the density of the mixture satisfies $\rho(\phi^{m+1}), \rho(\Pi_1^h \phi^{m+1}) \in [\rho_1, \rho_2]$ in Ω.*

The following Lemma is a technical result that we are going to use when computing the discrete energy law.

Lemma 3.7. *The following expression holds*

$$a_h^{upw}(\mathbf{u}^{m+1}; \phi^{m+1}, \Pi_0 \mu^{m+1}) + c_h(\phi^{m+1}, \Pi_0 \mu^{m+1}, \mathbf{u}^{m+1}) + s_h^2(\mathbf{u}^{m+1}, \phi^{m+1}, \Pi_0 \mu^{m+1}, \mathbf{u}^{m+1}) = 0. \quad (22)$$

Proof. First, notice that we can rewrite the term $a_h^{\text{upw}}(\mathbf{u}^{m+1}; \phi^{m+1}, \Pi_0 \mu^{m+1})$ as follows

$$a_h^{\text{upw}}(\mathbf{u}^{m+1}; \phi^{m+1}, \Pi_0 \mu^{m+1}) = \sum_{e \in \mathcal{E}_h} \int_e (\mathbf{u}^{m+1} \cdot \mathbf{n}_e) \{\!\{\phi^{m+1}\}\!\} [\![\Pi_0 \mu^{m+1}]\!]$$

$$+ \frac{1}{2} \sum_{e \in \mathcal{E}_h^i} \int_e |\mathbf{u}^{m+1} \cdot \mathbf{n}_e| [\![\phi^{m+1}]\!] [\![\Pi_0 \mu^{m+1}]\!].$$

Then, by definition and due to $\phi^{m+1} \in \mathbb{P}_0^{\text{disc}}(\mathcal{T}_h)$,

$$c_h(\phi^{m+1}, \Pi_0 \mu^{m+1}, \mathbf{u}^{m+1}) = -\int_\Omega (\nabla \cdot \mathbf{u}^{m+1}) \phi^{m+1} \Pi_0 \mu^{m+1}$$

$$- \sum_{e \in \mathcal{E}_h} \int_e (\mathbf{u}^{m+1} \cdot \mathbf{n}_e) \{\!\{\phi^{m+1}\}\!\} [\![\Pi_0 \mu^{m+1}]\!],$$

$$s_h^2(\mathbf{u}^{m+1}, \phi^{m+1}, \Pi_0 \mu^{m+1}, \mathbf{u}^{m+1}) = -\frac{1}{2} \sum_{e \in \mathcal{E}_h^i} \int_e |\mathbf{u}^{m+1} \cdot \mathbf{n}_e| [\![\phi^{m+1}]\!] [\![\Pi_0 \mu^{m+1}]\!].$$

Finally, using (10b),

$$c_h(\phi^{m+1}, \Pi_0 \mu^{m+1}, \mathbf{u}^{m+1}) = -\sum_{e \in \mathcal{E}_h} \int_e (\mathbf{u}^{m+1} \cdot \mathbf{n}_e) \{\!\{ \phi^{m+1} \}\!\} [\![\Pi_0 \mu^{m+1}]\!] ,$$

what yields (22). □

Theorem 3.8 (Discrete energy law). *The following discrete energy law holds:*

$$\delta_t E(\mathbf{u}^{m+1}, \Pi_1^h \phi^{m+1}) + 2 \left(\eta(\phi^{m+1}) \mathbf{Du}^{m+1}, \mathbf{Du}^{m+1} \right) + b_h^{upw}(-\nabla_\mathbf{n}^0 \mu^{m+1}; M(\phi^{m+1}), \Pi_0 \mu^{m+1})$$

$$+ \frac{\Delta t}{2} \int_\Omega \rho(\Pi_1^h \phi^m) |\delta_t \mathbf{u}^{m+1}|^2 + \frac{\Delta t \lambda \varepsilon}{2} \int_\Omega |\delta_t \nabla \Pi_1^h \phi^{m+1}|^2$$

$$+ \frac{\lambda}{\varepsilon} \int_\Omega \left(f(\Pi_1^h \phi^{m+1}, \Pi_1^h \phi^m) \delta_t \Pi_1^h \phi^{m+1} - F(\Pi_1^h \phi^{m+1}) \right) = 0, \tag{23}$$

where the energy functional $E(\mathbf{u}, \phi)$ is defined in (6).

Proof. First, take $\overline{\mathbf{u}} = \mathbf{u}^{m+1}$ and $\overline{p} = p^{m+1}$ in (10a)–(10b). Consider that

$$\left(\rho(\Pi_1^h \phi^m) \delta_t \mathbf{u}^{m+1}, \mathbf{u}^{m+1} \right) = \frac{1}{2} \int_\Omega \rho(\Pi_1^h \phi^m) \delta_t |\mathbf{u}^{m+1}|^2 + \frac{\Delta t}{2} \int_\Omega \rho(\Pi_1^h \phi^m) |\delta_t \mathbf{u}^{m+1}|^2, \tag{24}$$

and, by definition of $s_h^1(\cdot, \cdot, \cdot, \cdot, \cdot, \cdot)$ given in (15),

$$\frac{1}{2} \int_\Omega \delta_t \left(\rho(\Pi_1^h \phi^{m+1}) \right) |\mathbf{u}^{m+1}|^2 = \left(\left[\left(\rho(\Pi_1^h \phi^m) u^m - \mathbf{J}_h^m \right) \cdot \nabla \right] \mathbf{u}^{m+1}, \mathbf{u}^{m+1} \right)$$

$$+ s_h^1(\mathbf{u}^{m+1}, \mathbf{u}^m, \Pi_1^h \phi^{m+1}, \Pi_1^h \phi^m, \mu^m, \mathbf{u}^{m+1}). \tag{25}$$

Then, using (24) and (25) we can arrive at the following expression

$$\delta_t \int_\Omega \rho(\Pi_1^h \phi^{m+1}) \frac{|\mathbf{u}^{m+1}|^2}{2} + \frac{\Delta t}{2} \int_\Omega \rho(\Pi_1^h \phi^m) |\delta_t \mathbf{u}^{m+1}|^2 + 2 \left(\eta(\phi^{m+1}) \mathbf{Du}^{m+1}, \mathbf{Du}^{m+1} \right)$$

$$+ c_h(\phi^{m+1}, \Pi_0 \mu^{m+1}, \mathbf{u}^{m+1}) + s_h^2(\mathbf{u}^{m+1}, \phi^{m+1}, \Pi_0 \mu^{m+1}, \mathbf{u}^{m+1}) = 0. \tag{26}$$

Now, if we test (10c)–(10d) with $\overline{\phi} = \Pi_0 \mu^{m+1}$ and $\overline{\mu} = \delta_t \Pi_1^h \phi^{m+1}$ and we add the resulting expressions and (26), we obtain, using (22),

$$\delta_t \int_\Omega \rho(\Pi_1^h \phi^{m+1}) \frac{|\mathbf{u}^{m+1}|^2}{2} + \frac{\Delta t}{2} \int_\Omega \rho(\Pi_1^h \phi^m) |\delta_t \mathbf{u}^{m+1}|^2 + 2 \left(\eta(\phi^{m+1}) \mathbf{Du}^{m+1}, \mathbf{Du}^{m+1} \right)$$

$$+ \left(\delta_t \phi^{m+1}, \Pi_0 \mu^{m+1} \right) + b_h^{upw}(-\nabla_\mathbf{n}^0 \mu^{m+1}; M(\phi^{m+1}), \Pi_0 \mu^{m+1}) + \lambda \varepsilon \left(\nabla \Pi_1^h \phi^{m+1}, \delta_t \nabla \Pi_1^h \phi^{m+1} \right)$$

$$+ \frac{\lambda}{\varepsilon} \left(f(\Pi_1^h \phi^{m+1}, \Pi_1^h \phi^m), \delta_t \Pi_1^h \phi^{m+1} \right) - \left(\mu^{m+1}, \delta_t \Pi_1^h \phi^{m+1} \right)_h = 0.$$

Finally, the following equalities

$$\left(\delta_t \phi^{m+1}, \Pi_0 \mu^{m+1} \right) = \left(\delta_t \phi^{m+1}, \mu^{m+1} \right) = \left(\delta_t \Pi_1^h \phi^{m+1}, \mu^{m+1} \right)_h,$$

$$\lambda \varepsilon \left(\nabla \Pi_1^h \phi^{m+1}, \delta_t \nabla \Pi_1^h \phi^{m+1} \right) = \frac{\lambda \varepsilon}{2} \delta_t \int_\Omega |\nabla \Pi_1^h \phi^{m+1}|^2 + \frac{\Delta t \lambda \varepsilon}{2} \int_\Omega |\delta_t \nabla \Pi_1^h \phi^{m+1}|^2,$$

yield (23). □

Using the definition of the upwind form $b_h^{\text{upw}}(\cdot; \cdot, \cdot)$ and the standard procedure for the convex-splitting technique (see e.g. [21, 26]), one can show the following Lemma.

Lemma 3.9. *The following two inequalities hold:*

$$b_h^{upw}(-\nabla_{\mathbf{n}}^0 \mu^{m+1}; M(\phi^{m+1}), \Pi_0 \mu^{m+1}) \geq 0, \tag{27}$$

$$\int_\Omega \left(f(\Pi_1^h \phi^{m+1}, \Pi_1^h \phi^m) \delta_t \Pi_1^h \phi^{m+1} - \delta_t F(\Pi_1^h \phi^{m+1}) \right) \geq 0. \tag{28}$$

The following result is a direct consequence of Theorem 3.8 and Lemma 3.9.

Corollary 3.10 (Discrete energy stability). *The scheme* (10) *satisfies*

$$\delta_t E(\mathbf{u}^{m+1}, \Pi_1^h \phi^{m+1}) + 2 \left(\eta(\phi^{m+1}) \mathbf{Du}^{m+1}, \mathbf{Du}^{m+1} \right) + b_h^{upw}(-\nabla_{\mathbf{n}}^0 \mu^{m+1}; M(\phi^{m+1}), \Pi_0 \mu^{m+1}) \leq 0. \tag{29}$$

In particular, scheme (10) *is unconditionally energy stable, i.e.,* $\delta_t E(\mathbf{u}^{m+1}, \Pi_1^h \phi^{m+1}) \leq 0.$

The scheme (10) is nonlinear so we will need to approximate its solution by means of an iterative procedure such as the nonsmooth Newton's method (see [15]).

However, the function $\text{sign}(\phi)$ that appears in the stabilization term $s_h^2(\cdot, \cdot, \cdot, \cdot)$ is not subdifferentiable at $\phi = 0$ and, although it is rare in practice that $\phi = 0$ holds exactly due to round-off errors, one might eventually find convergence issues.

In this case, several approaches can be carried out to improve the convergence of the algorithm. For instance, one may use an iterative procedure that does not rely on the Jacobian of the whole system such as a fixed point algorithm. Conversely, if we want to use a higher order procedure depending on the Jacobian like the nonsmooth Newton's method, one may avoid the use of the sign() function regularizing the term $s_h^2(\cdot, \cdot, \cdot, \cdot)$ as follows

$$s_h^{2,\delta}(\mathbf{u}, \phi, \mu, \overline{\mathbf{u}}) := \frac{1}{2} \sum_{e \in \mathcal{E}_h^i} \int_e (\overline{\mathbf{u}} \cdot \mathbf{n}_e) \frac{\mathbf{u} \cdot \mathbf{n}_e}{|\mathbf{u} \cdot \mathbf{n}_e| + \delta} [\![\Pi_0 \mu]\!] [\![\phi]\!], \tag{30}$$

for $\delta > 0$ small. This modification preserves the mass conservation and the point-wise bounds but introduces a modification in the discrete energy law, see Theorem 3.11.

The following result can be proved using the same procedure in Theorem 3.8 and Corollary 3.10.

Theorem 3.11. *If we regularize the stabilization term* $s_h^2(\cdot, \cdot, \cdot, \cdot)$ *in the equation* (10a), *using* $s_h^{2,\delta}(\cdot, \cdot, \cdot, \cdot)$ *defined in* (30) *for a certain* $\delta > 0$, *the following discrete energy law holds:*

$$\delta_t E(\mathbf{u}^{m+1}, \Pi_1^h \phi^{m+1}) + 2 \left(\eta(\phi^{m+1}) \mathbf{Du}^{m+1}, \mathbf{Du}^{m+1} \right) + b_h^{upw}(-\nabla_{\mathbf{n}}^0 \mu^{m+1}; M(\phi^{m+1}), \Pi_0 \mu^{m+1})$$

$$\leq -\frac{\delta}{2} \sum_{e \in \mathcal{E}_h^i} \int_e \frac{|\mathbf{u}^{m+1} \cdot \mathbf{n}_e|}{|\mathbf{u}^{m+1} \cdot \mathbf{n}_e| + \delta} [\![\Pi_0 \mu^{m+1}]\!] [\![\phi^{m+1}]\!]. \tag{31}$$

4 Decoupled bound-preserving scheme

Now, we develop a decoupled approximation of the model (1) that reduces significantly the computational effort with respect to the previous coupled approach (10), while still preserving the mass conservation and the point-wise bounds.

Nonetheless, as a tradeoff, in this case it is not clear whether a discrete energy law directly holds even for the corresponding time semidiscrete scheme (32) given below. In fact, numerical experiments suggest that, in general, the decoupled approximation may become energy unstable for certain choice of the parameters, see Test (5.2). Hence, we will not focus on the energy stability of decoupled fully discrete schemes and we leave this study for a future work.

4.1 Time discrete scheme

For clarity in the exposition, we are going to introduce first the time semidiscretization used to decouple the equations. In particular, we apply a rotational pressure-correction method based on the work in [31] to decouple the fluid equations.

Consider the following steps:

Step 1: given $(\phi^m, \mu^m, \mathbf{u}^m, p^m)$ compute $\mathbf{v}^{m+1}$ satisfying

$$\rho(\phi^m)\frac{\mathbf{v}^{m+1} - \mathbf{u}^m}{\Delta t} + \left[(\rho(\phi^m)\mathbf{v}^m - \rho_{dif}M(\phi^m)\nabla\mu^m) \cdot \nabla\right]\mathbf{v}^{m+1}$$
$$-2\nabla \cdot (\eta(\phi^m)\mathbf{D}\mathbf{v}^{m+1}) + \nabla p^m + \phi^m\nabla\mu^m = 0 \quad \text{in } \Omega, \tag{32a}$$

$$\mathbf{v}^{m+1} = 0 \quad \text{on } \partial\Omega. \tag{32b}$$

Step 2: given $(\phi^m, \mathbf{v}^{m+1})$ compute τ^{m+1}, with $\int_\Omega \tau^{m+1} = 0$ and satisfying

$$-\nabla \cdot \left(\frac{1}{\rho(\phi^m)}\nabla\tau^{m+1}\right) = -\frac{1}{\Delta t}\nabla \cdot \mathbf{v}^{m+1}, \quad \text{in } \Omega, \tag{32c}$$

$$\nabla\tau^{m+1} \cdot \mathbf{n} = 0, \quad \text{on } \partial\Omega. \tag{32d}$$

Step 3: given $(\phi^m, \tau^{m+1}, \mathbf{v}^{m+1}, p^m)$ compute $(p^{m+1}, \mathbf{u}^{m+1})$ satisfying

$$p^{m+1} = p^m + \tau^{m+1} - 2\eta(\phi^m)\nabla \cdot \mathbf{v}^{m+1}, \tag{32e}$$

$$\mathbf{u}^{m+1} = \mathbf{v}^{m+1} - \frac{\Delta t}{\rho(\phi^m)}\nabla\tau^{m+1}, \tag{32f}$$

where p^{m+1} is post-processed to ensure the 0-mean constraint. Note that the velocity $\mathbf{u}^{m+1}$ is incompressible and $\mathbf{u}^{m+1} \cdot \mathbf{n} = 0$ on $\partial\Omega$.

Step 4: given $(\phi^m, \mathbf{u}^{m+1})$, compute (ϕ^{m+1}, μ^{m+1}) satisfying:

$$\delta_t\phi^{m+1} + \nabla \cdot (\phi^{m+1}\mathbf{u}^{m+1}) - \nabla \cdot (M(\phi^{m+1})\nabla\mu^{m+1}) = 0 \quad \text{in } \Omega, \tag{32g}$$

$$-\lambda\varepsilon\Delta\phi^{m+1} + \frac{\lambda}{\varepsilon}f(\phi^{m+1}, \phi^m) - \mu^{m+1} = 0 \quad \text{in } \Omega, \tag{32h}$$

$$\nabla\phi^{m+1} \cdot \mathbf{n} = M(\phi^{m+1})\nabla\mu^{m+1} \cdot \mathbf{n} = 0 \quad \text{on } \partial\Omega, \tag{32i}$$

where $f(\cdot, \cdot)$ is defined in (11).

Notice that this projection method only leads to an inaccurate boundary condition on the velocity variable $\mathbf{u}^{m+1}$ in the tangential direction due to the terms depending on $\nabla \tau^{m+1}$ in (32f), in fact, one only has the so-called slip boundary condition $\mathbf{u}^{m+1} \cdot \mathbf{n} = 0$ on $\partial\Omega$. For further insight on this issue with projection methods, see, for instance, [24].

4.2 Fully discrete scheme

We will use the well known SIP method (see [17, 34]) to discretize the term $-\nabla \cdot (\kappa \nabla \tau)$ in (32c), where $\kappa = \kappa(x) \in L^\infty(\Omega)$ with that $\kappa \geq C > 0$ in Ω, by means of the bilinear form

$$a_h^{\text{sip},\sigma}(\kappa; \tau, \overline{\tau}) := \int_\Omega \kappa \nabla\tau \cdot \nabla\overline{\tau} - \left(\sum_{e \in \mathcal{E}_h^i} \int_e \{\!\{\kappa\nabla\tau\}\!\} \cdot \mathbf{n}_e \, [\![\overline{\tau}]\!] + \sum_{e \in \mathcal{E}_h^i} \int_e \{\!\{\kappa\nabla\overline{\tau}\}\!\} \cdot \mathbf{n}_e \, [\![\tau]\!] \right) + \sum_{e \in \mathcal{E}_h^i} \int_e \frac{\sigma}{|e|} \, [\![\tau]\!] \, [\![\overline{\tau}]\!], \tag{33}$$

where $\sigma > 0$ is a parameter large enough to ensure the coercivity of the bilinear form $a_h^{\text{sip},\sigma}(\kappa; \cdot, \cdot)$.

Then, we propose the following decoupled fully discrete scheme based on the previous time-discrete approach. In order to simplify the notation, we will denote the fully discrete functions the same way as the time-semidiscrete functions in (32).

Step 1: given $(\phi^m, \mu^m, \mathbf{u}^m, p^m) \in \mathbb{P}_0^{\text{disc}}(\mathcal{T}_h) \times \mathbb{P}_1^{\text{cont}}(\mathcal{T}_h) \times \mathcal{U}_h \times \mathcal{P}_h$ compute $\mathbf{v}^{m+1} \in \mathcal{V}_h$ satisfying

$$\left(\rho(\phi^m) \frac{\mathbf{v}^{m+1} - \mathbf{u}^m}{\Delta t}, \overline{\mathbf{v}} \right) + \left([(\rho(\phi^m)\mathbf{v}^m - \rho_{dif} M(\phi^m)\nabla\mu^m) \cdot \nabla] \, \mathbf{v}^{m+1}, \overline{\mathbf{v}} \right)$$

$$+ \left(2\eta(\phi^m)\mathbf{D}\mathbf{v}^{m+1}, \mathbf{D}\overline{\mathbf{v}} \right) - (p^m, \nabla \cdot \overline{\mathbf{v}}) + (\phi^m \nabla\mu^m, \overline{\mathbf{v}}) = 0, \quad \forall \overline{\mathbf{v}} \in \mathcal{V}_h, \tag{34a}$$

with $\mathbf{v}^{m+1} = 0$ on $\mathcal{E}_h^b$.

Step 2: given $(\phi^m, \mathbf{v}^{m+1}) \in \mathbb{P}_0^{\text{disc}}(\mathcal{T}_h) \times \mathcal{V}_h$ compute $\tau^{m+1} \in \mathbb{P}_1^{\text{disc}}(\mathcal{T}_h)$ satisfying

$$a_h^{\text{sip},\sigma}(1/\rho(\phi^m); \tau^{m+1}, \overline{\tau}) = -\frac{1}{\Delta t} \left(\nabla \cdot \mathbf{v}^{m+1}, \overline{\tau} \right), \quad \forall \overline{\tau} \in \mathbb{P}_1^{\text{disc}}(\mathcal{T}_h). \tag{34b}$$

Step 3: given $(\phi^m, \tau^{m+1}, \mathbf{v}^{m+1}, p^m) \in \mathbb{P}_0^{\text{disc}}(\mathcal{T}_h) \times \mathbb{P}_1^{\text{disc}}(\mathcal{T}_h) \times \mathcal{V}_h \times \mathcal{P}_h$ compute $p^{m+1} \in \mathcal{P}_h$ as follows

$$\left(p^{m+1}, \overline{p} \right) = (p^m, \overline{p}) + \left(\tau^{m+1}, \overline{p} \right) - 2 \left(\eta(\phi^m)\nabla \cdot \mathbf{v}^{m+1}, \overline{p} \right) \quad \forall \overline{p} \in \mathcal{P}_h, \tag{34c}$$

Step 4: given $(\phi^m, \mathbf{v}^{m+1}) \in \mathbb{P}_0^{\text{disc}}(\mathcal{T}_h) \times \mathcal{V}_h$ compute $(\phi^{m+1}, \mu^{m+1}) \in \mathbb{P}_0^{\text{disc}}(\mathcal{T}_h) \times \mathbb{P}_1^{\text{cont}}(\mathcal{T}_h)$ satisfying:

$$\left(\delta_t \phi^{m+1}, \overline{\phi} \right) + a_h^{\text{upw}}(\widetilde{\mathbf{u}}^{m+1}; \phi^{m+1}, \overline{\phi}) + b_h^{\text{upw}}(-\nabla_{\mathbf{n}}\mu^{m+1}; M(\phi^{m+1}), \overline{\phi}) = 0, \quad \forall \overline{\phi} \in \mathbb{P}_0^{\text{disc}}(\mathcal{T}_h), \tag{34d}$$

$$\lambda \varepsilon \left(\nabla(\Pi^h \phi^{m+1}), \nabla\overline{\mu} \right) + \frac{\lambda}{\varepsilon} \left(f(\phi^{m+1}, \phi^m), \overline{\mu} \right) - \left(\mu^{m+1}, \overline{\mu} \right) = 0, \quad \forall \overline{\mu} \in \mathbb{P}_1^{\text{cont}}(\mathcal{T}_h), \tag{34e}$$

where the velocity $\widetilde{\mathbf{u}}^{m+1}$ in (34d) is defined on every $e \in \mathcal{E}_h^i$ as follows

$$\widetilde{\mathbf{u}}_{|e}^{m+1} \cdot \mathbf{n}_e := \{\!\{\mathbf{u}^{m+1}\}\!\} \cdot \mathbf{n}_e + \Delta t \frac{\sigma}{|e|} \, [\![\tau^{m+1}]\!], \tag{34f}$$

16

with

$$\mathbf{u}^{m+1} = \mathbf{v}^{m+1} - \frac{\Delta t}{\rho(\phi^m)} \nabla \tau^{m+1}. \tag{34g}$$

By construction, this modified velocity $\widetilde{\mathbf{u}}^{m+1}$ is locally incompressible. Hence, the point-wise bounds $\phi^{m+1}, \Pi^h \phi^{m+1} \in [-1, 1]$ will be preserved, see Proposition 4.2 and Theorem 4.4 below. Note that, for every $e \in \mathcal{E}_h^{\mathrm{i}}$, the stabilization term $\Delta t(\sigma/|e|) [\![\tau^{m+1}]\!]$ is consistent and vanishes as $\Delta t, h \to 0$.

The upwind forms $a_h^{\mathrm{upw}}(\mathbf{u}; \phi, \overline{\phi})$ and $b_h^{\mathrm{upw}}(-\nabla_\mathbf{n} \mu; M(\phi), \overline{\phi})$ have been already defined in (14) and (19), respectively.

We have denoted $(\mathcal{V}_h, \mathcal{U}_h, \mathcal{P}_h)$ to any triple of discrete spaces such that $\mathcal{U}_h = \mathcal{V}_h + \mathbb{P}_0^{\mathrm{disc}}(\mathcal{T}_h)^d$ with $\mathcal{V}_h \subset (\mathcal{C}^0(\overline{\Omega}) \cap H_0^1(\Omega))^d$.

In this case, the triple $(\mathcal{V}_h, \mathcal{U}_h, \mathcal{P}_h)$ needs to satisfy $\mathcal{V}_h \subset (\mathcal{C}^0(\overline{\Omega}) \cap H_0^1(\Omega))^d$ in order to strongly impose the no-slip boundary condition on $\mathbf{v}^{m+1}$ and $\mathcal{U}_h = \mathcal{V}_h + \mathbb{P}_0^{\mathrm{disc}}(\mathcal{T}_h)$, directly derived from equation (34g), to preserve the local incompressibility of the variable $\mathbf{u}^{m+1}$ (see Lemma 4.1).

Although we do not know if the solution of this decoupled scheme (34) satisfies any discrete energy law, in case that we achieve estimates for the velocity $\mathbf{u}^{m+1}$, it is preferable to choose an inf-sup compatible pair of spaces $(\mathcal{V}_h, \mathcal{P}_h)$ as was mentioned in Section 3. For more information on the inf-sup condition for projection methods we refer the reader to [24, 25].

Again, as in the fully coupled approximation scheme (10), the error bounds are expected to be determined by the lowest accuracy approximation of the phase-field function given by $\mathbb{P}_0^{\mathrm{disc}}(\mathcal{T}_h)$.

To start the algorithm we take again $\phi^0 = \Pi_0 \phi_0$ hence $\phi^0 \in [-1, 1]$. Also, we take $\mathbf{u}^0$ as the projection of $\mathbf{u}_0$ on $\mathcal{V}_h$ and $p^0 = 0$.

Since we are not certain about if an energy law can be derived for the solution of the semidiscrete scheme (32), we have omitted in this case the constraints and stabilization terms needed for the fully coupled scheme (10) to be energy-stable. Indeed, we have not used the approximation of the normal derivative of the chemical potential (20) in (34d) and, consequently, we can omit Hypothesis 1 for the decoupled scheme (34). Therefore, the approximation given by the decoupled scheme (34) can be computed in more general meshes than its coupled counterpart (10).

Moreover, since only the equation (34d) is nonlinear in the decoupled fully discrete scheme (34), we will only need to use an iterative procedure such as Newton's method to approximate the solution in Step 1. This improvement reduces significantly the computational cost with respect to the fully coupled scheme (10) which requires an iterative procedure to be carried out for the whole system.

4.2.1 Properties of the scheme (34)

In this subsection, we will only show the proof of the local incompressibility of $\mathbf{u}^{m+1}$ and we will just state the other results as they are analogous to the ones in Subsection 3.2.2.

Lemma 4.1 (Approximated local incompressibility). *The velocity variable $\mathbf{u}^{m+1}$ computed from* (34g) *is approximately locally incompressible in the following sense:*

$$\sum_{e \in \mathcal{E}_h^i} \int_e \{\!\{\mathbf{u}^{m+1}\}\!\} \cdot \mathbf{n}_e [\![\overline{\varphi}]\!] = -\Delta t \sum_{e \in \mathcal{E}_h^i} \int_e \frac{\sigma}{|e|} [\![\tau^{m+1}]\!] [\![\overline{\varphi}]\!], \quad \forall \overline{\varphi} \in \mathbb{P}_0^{disc}(\mathcal{T}_h), \tag{35}$$

where the right hand side of (35) *tends to 0 as $\Delta t, h \to 0$.*

Proof. Let $\overline{\varphi} \in \mathbb{P}_0^{\text{disc}}(\mathcal{T}_h)$. Taking the (broken) divergence of (34g) and testing by $\overline{\varphi}$ we arrive at

$$\left(\nabla \cdot \mathbf{u}^{m+1}, \overline{\varphi}\right) = \left(\nabla \cdot \mathbf{v}^{m+1}, \overline{\varphi}\right) - \left(\nabla \cdot \left(\frac{\Delta t}{\rho(\phi^m)} \nabla \tau^{m+1}\right), \overline{\varphi}\right). \tag{36}$$

Now, substituting (34b) into (36),

$$\left(\nabla \cdot \mathbf{u}^{m+1}, \overline{\varphi}\right) = -\Delta t \left[a_h^{\text{sip},\sigma}(1/\rho(\phi^m); \tau^{m+1}, \overline{\varphi}) + \left(\nabla \cdot \left(\frac{1}{\rho(\phi^m)} \nabla \tau^{m+1}\right), \overline{\varphi}\right)\right]. \tag{37}$$

Since $\overline{\varphi}$ is piecewise constant in $\mathcal{T}_h$,

$$a_h^{\text{sip},\sigma}(1/\rho(\phi^m); \tau^{m+1}, \overline{\varphi}) = -\sum_{e \in \mathcal{E}_h^i} \int_e \{\!\{(1/\rho(\phi^m))\nabla \tau^{m+1}\}\!\} \cdot \mathbf{n}_e [\![\overline{\varphi}]\!] + \sum_{e \in \mathcal{E}_h^i} \int_e \frac{\sigma}{|e|} [\![\tau^{m+1}]\!] [\![\overline{\varphi}]\!],$$

integrating by parts, we obtain

$$\left(\nabla \cdot \left(\frac{1}{\rho(\phi^m)} \nabla \tau^{m+1}\right), \overline{\varphi}\right) = \sum_{e \in \mathcal{E}_h} \int_e \{\!\{(1/\rho(\phi^m))\nabla \tau^{m+1}\}\!\} \cdot \mathbf{n}_e [\![\overline{\varphi}]\!]$$
$$+ \sum_{e \in \mathcal{E}_h} \int_e [\![(1/\rho(\phi^m))\nabla \tau^{m+1}]\!] \cdot \mathbf{n}_e \{\!\{\overline{\varphi}\}\!\}.$$

Hence, returning to (37) and using (34g) and that $[\![\mathbf{v}^{m+1}]\!] = 0$ on $\mathcal{E}_h$ due to the choice of $\mathcal{V}_h$, we have

$$\left(\nabla \cdot \mathbf{u}^{m+1}, \overline{\varphi}\right) = -\Delta t \sum_{e \in \mathcal{E}_h} \int_e [\![(1/\rho(\phi^m))\nabla \tau^{m+1}]\!] \cdot \mathbf{n}_e \{\!\{\overline{\varphi}\}\!\} - \Delta t \sum_{e \in \mathcal{E}_h^b} \int_e (1/\rho(\phi^m))(\nabla \tau^{m+1} \cdot \mathbf{n}_e)\overline{\varphi}$$

$$- \Delta t \sum_{e \in \mathcal{E}_h^i} \int_e \frac{\sigma}{|e|} [\![\tau^{m+1}]\!] [\![\overline{\varphi}]\!]$$

$$= \sum_{e \in \mathcal{E}_h} \int_e [\![\mathbf{u}^{m+1}]\!] \cdot \mathbf{n}_e \{\!\{\overline{\varphi}\}\!\} - \Delta t \sum_{e \in \mathcal{E}_h^b} \int_e (1/\rho(\phi^m))(\nabla \tau^{m+1} \cdot \mathbf{n}_e)\overline{\varphi}$$

$$- \Delta t \sum_{e \in \mathcal{E}_h^i} \int_e \frac{\sigma}{|e|} [\![\tau^{m+1}]\!] [\![\overline{\varphi}]\!]$$

$$= \sum_{e \in \mathcal{E}_h} \int_e [\![\mathbf{u}^{m+1}]\!] \cdot \mathbf{n}_e \{\!\{\overline{\varphi}\}\!\} + \sum_{e \in \mathcal{E}_h^b} (\mathbf{u}^{m+1} \cdot \mathbf{n}_e)\overline{\varphi} - \Delta t \sum_{e \in \mathcal{E}_h^i} \int_e \frac{\sigma}{|e|} [\![\tau^{m+1}]\!] [\![\overline{\varphi}]\!]. \tag{38}$$

Now, integrate by parts the left-hand side of (38),

$$\left(\nabla \cdot \mathbf{u}^{m+1}, \overline{\varphi}\right) = \sum_{e \in \mathcal{E}_h} \int_e \{\!\{\mathbf{u}^{m+1}\}\!\} \cdot \mathbf{n}_e [\![\overline{\varphi}]\!] + \sum_{e \in \mathcal{E}_h} \int_e [\![\mathbf{u}^{m+1}]\!] \cdot \mathbf{n}_e \{\!\{\overline{\varphi}\}\!\}. \tag{39}$$

Consequently, due to (38) and (39), we arrive at (35). □

The following result is a direct consequence of the previous lemma.

Proposition 4.2 (Local incompressibility). *The modified velocity $\widetilde{\mathbf{u}}^{m+1}$ defined in (34f) is locally incompressible in the sense that*

$$\sum_{e \in \mathcal{E}_h^i} \int_e \widetilde{\mathbf{u}}^{m+1} \cdot \mathbf{n}_e \, [\![\overline{\varphi}]\!] = 0, \quad \forall \overline{\varphi} \in \mathbb{P}_0^{disc}(\mathcal{T}_h). \tag{40}$$

The proofs of the remaining following results are analogous to those shown in Section 3.2.2 for the coupled approach (10).

Proposition 4.3 (Mass conservation). *The mass of the phase-field variable and its regularization are conserved, i.e.,*

$$\int_\Omega \phi^{m+1} = \int_\Omega \phi^m, \quad \int_\Omega \Pi_1^h \phi^{m+1} = \int_\Omega \Pi_1^h \phi^m.$$

As a consequence, since $\rho(\phi)$ is linear with respect to ϕ, the mass of the mixture is also conserved,

$$\int_\Omega \rho(\phi^{m+1}) = \int_\Omega \rho(\phi^m), \quad \int_\Omega \rho(\Pi_1^h \phi^{m+1}) = \int_\Omega \rho(\Pi_1^h \phi^m).$$

Theorem 4.4 (Point-wise bounds of the phase-field variable). *Provided that $\phi^m \in [-1,1]$ in Ω, any solution ϕ^{m+1} and its $\mathbb{P}_1^{cont}(\mathcal{T}_h)$-regularization $\Pi_1^h \phi^{m+1}$ in (34d) satisfy $\phi^{m+1}, \Pi_1^h \phi^{m+1} \in [-1,1]$ in Ω.*

Corollary 4.5 (Point-wise bounds of the mixture density). *Provided that $\rho(\phi^m) \in [\rho_1, \rho_2]$ in Ω, the density of the mixture $\rho(\phi^{m+1})$ or $\rho(\Pi_1^h \phi^{m+1})$ in (34) satisfy $\rho(\phi^{m+1}), \rho(\Pi_1^h \phi^{m+1}) \in [\rho_1, \rho_2]$ in Ω.*

In this case, we cannot guarantee an energy-stability property for the decoupled fully discrete scheme (34). In fact, it seems that this approach may become unstable for a certain choice of the parameters as shown by numerical experiments (see Test 5.2 below). However, this approach should not be dismissed as it is still an efficient alternative that works in many cases allowing us to compute the results of certain tests up to 75% faster than with the coupled counterpart (10). In practice, one can check when this scheme is not energy stable by computing the discrete energy. When this discrete energy diverges, leading to an unstable approximation, we can switch to the more robust coupled counterpart to compute the approximation. An in-depth comparison between both approaches through some numerical experiments is shown in Section 5.

Notice that we have maintained the convection term semi-implicitly in the fluid equation (34a) as in the fully coupled approximation (10a). We will see numerically that the approximation obtained is energy stable in many situations, see Tests 5.3 and 5.4 below, although it is unstable in Test 5.2, see Figures 4 and 5 below. But, if we take this convection term fully explicitly, then the approximation tends to become energy unstable even for the Tests 5.3 and 5.4.

5 Numerical experiments

We have carried out the following numerical experiments in the spatial domain $\Omega = [-0.5, 0.5]^2$. Moreover, we have set the following values of the parameters $\varepsilon = 0.01$, $\lambda = 0.01$, $\rho_1 = 1$ and $\rho_2 = 100$, unless otherwise specified. Also, the penalty parameter σ has been chosen as $\sigma = 4$ in (34), although other choices might have been possible.

Following the Remark 3.1, we have chosen the pair of "inf-sup" stable spaces $(\mathcal{U}_h, \mathcal{P}_h) = ((\mathbb{P}_2^{\text{bubble}}(\mathcal{T}_h) \cap H_0^1(\Omega))^d, \mathbb{P}_1^{\text{disc}}(\mathcal{T}_h))$ for the coupled scheme (10) and $(\mathcal{V}_h, \mathcal{P}_h) = ((\mathbb{P}_2^{\text{bubble}}(\mathcal{T}_h) \cap H_0^1(\Omega))^d, \mathbb{P}_1^{\text{disc}}(\mathcal{T}_h))$ regarding the decoupled approach (34), where $\mathcal{U}_h = (\mathbb{P}_2^{\text{bubble}}(\mathcal{T}_h) \cap H_0^1(\Omega))^d + \mathbb{P}_0^{\text{disc}}(\mathcal{T}_h)^d$.

To compute the approximations we have used the finite element library FEniCSx (see [5, 35, 36]) coupled with PyVista for the visualization of the results (see [40]). The source code for our implementation is hosted on GitHub[1].

On the one hand, an iterative Newton solver has been used to approximate the nonlinear problem. In this sense, the modified stabilization term $s_h^{2,\delta}(\cdot, \cdot, \cdot,)$ with $\delta = 10^{-6}$ has been used in the coupled scheme (10) to avoid convergence issues.

On the other hand, we have used the default iterative linear solver, GMRES (generalized minimal residual method), and preconditioner, computed using an incomplete LU factorization (ILU), of PETSc (see [8, 16]) for solving the resulting linear systems except (34a). In the case of (34a), this combination provided some instabilities in several examples. Therefore, we opted for a different approach and used an LU parallel solver implemented in MUMPS, [6, 7], for (34a), which provided much more accurate results shown in the figures below.

Remark 5.1. *In the case of the decoupled approach* (34), *enforcing the 0-mean constraint on the approximation of the potential τ is rather straightforward as the linear Krylov solvers can handle singular matrices and provide a solution of the linear system. Therefore, we compute a solution of the linear system and then post-process it so that it satisfies the constraint.*

However, we must be careful when dealing with an ill-posed nonlinear problem if we want Newton's method to converge. To overcome this issue in the case of the coupled approximation (10), *we have added a penalty term $\xi(p^{m+1}, \overline{p})$ to the LHS of* (10b) *with ξ very small (in practice, we have chosen $\xi = 10^{-10}$). In this way, we enforce the 0-mean constraint on the approximation of p and Newton's method does converge. In fact, a posteriori, we can check that this additional term has not severely affected the approximation obtained in two different manners. On the one hand, taking into account the $\|\cdot\|_\infty$ of the approximation of p we observe that the term ξp has been at most of order 10^{-5}. On the other hand, the point-wise bounds have been preserved despite the crucial role that the local incompressibility constraint* (12) *plays in Theorem 3.5.*

---

[1] https://github.com/danielacos/Papers-src

Certainly, many other ways of enforcing the 0-mean pressure constraint in the coupled nonlinear system can be explored.

In all the figures shown in this section, we plot both the phase field variable (in red/blue) and the following scaled vector field (in white)

$$\mathbf{u}_s^{m+1} = \begin{cases} \dfrac{5 \cdot 10^{-2}}{\|\mathbf{u}^{m+1}\|_{L^\infty(\Omega)}} \mathbf{u}^{m+1}, & \text{if } \|\mathbf{u}^{m+1}\|_{L^\infty(\Omega)} \geq 5 \cdot 10^{-2}, \\ \mathbf{u}^{m+1}, & \text{otherwise.} \end{cases}$$

5.1 Accuracy test

In this case, we define the following initial conditions

$$\phi_0(x,y) = 2 \tanh\left(\frac{(0.25 - \sqrt{(x-0.1)^2 + (y-0.1)^2})_\oplus}{\sqrt{2}\varepsilon} \right.$$
$$\left. + \frac{(0.15 - \sqrt{(x+0.15)^2 + (y+0.15)^2})_\oplus}{\sqrt{2}\varepsilon} \right) - 1.0,$$
$$\mathbf{u}_0(x,y) = \chi(y(0.16 - (x^2+y^2))_\oplus, -x(0.16 - (x^2+y^2))_\oplus),$$

with $\chi = 1$, which are plotted in Figure 1.
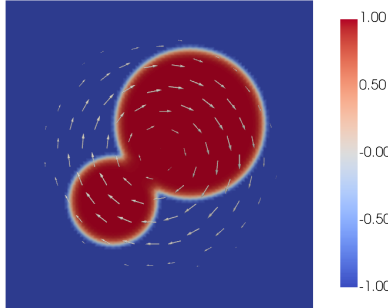
Figure 1: Initial condition of Tests 5.1 and 5.2.

We conduct a preliminary convergence test in which we compare a reference solution given by each of the coupled, (10), and decoupled, (34), approaches in a very refined mesh ($h \approx 7 \cdot 10^{-3}$) with the approximation given by the same approach in a less refined mesh. In this way, with $\Delta t = 10^{-5}$ fixed, we can remove the error introduced by the time discretization in each of the different schemes. In any case, we would like to emphasize that such a test for these sophisticated schemes involving several different discrete spaces and projection operators is nontrivial and the results obtained only provide an estimation of the possible order of convergence of the proposed approximations.

The results of the test at $T = 5 \cdot 10^{-4}$ are shown in Tables 1 and 2, where similar orders of convergence have been achieved for both schemes (10) and (34). It is worth mentioning that, as

Variable	Scheme	$h \approx 2.36 \cdot 10^{-2}$	$3h/4 \approx 1.77 \cdot 10^{-2}$		$4h/7 \approx 1.35 \cdot 10^{-2}$		$h/2 \approx 1.18 \cdot 10^{-2}$	
		Error	Error	**Order**	Error	**Order**	Error	**Order**
$\Pi_1^h \phi$	Coupled	$8.48e-03$	$5.40e-03$	1.57	$3.38e-03$	1.73	$2.62e-03$	1.89
	Decoupled	$8.80e-03$	$5.59e-03$	1.58	$3.21e-03$	2.05	$2.54e-03$	1.74
$\mathbf{u}$	Coupled	$5.91e-04$	$4.89e-04$	0.66	$3.31e-04$	1.44	$2.43e-04$	2.30
	Decoupled	$2.57e-04$	$6.98e-05$	4.53	$3.09e-05$	3.01	$2.46e-05$	1.69
p	Coupled	$2.24e-01$	$1.14e-01$	2.35	$5.47e-02$	2.71	$4.37e-02$	1.67
	Decoupled	$9.26e-02$	$1.90e-02$	5.51	$1.14e-02$	1.89	$8.87e-03$	1.86

Table 1: Errors and convergence orders at $T = 5 \cdot 10^{-4}$ in $\|\cdot\|_{L^2(\Omega)}$.

Variable	Scheme	$h \approx 2.36 \cdot 10^{-2}$	$3h/4 \approx 1.77 \cdot 10^{-2}$		$3h/5 \approx 1.41 \cdot 10^{-2}$		$h/2 \approx 1.18 \cdot 10^{-2}$	
		Error	Error	**Order**	Error	**Order**	Error	**Order**
$\Pi_1^h \phi$	Coupled	$1.22e+00$	$1.17e+00$	0.15	$9.12e-01$	0.92	$8.09e-01$	0.89
	Decoupled	$1.34e+00$	$1.25e+00$	0.24	$9.43e-01$	1.04	$8.31e-01$	0.94
$\mathbf{u}$	Coupled	$9.61e-02$	$7.98e-02$	0.65	$4.90e-02$	1.80	$3.75e-02$	1.99
	Decoupled	$2.06e-02$	$8.82e-03$	2.95	$4.03e-03$	2.89	$3.30e-03$	1.48

Table 2: Errors and convergence orders at $T = 5 \cdot 10^{-4}$ in $\|\cdot\|_{H^1(\Omega)}$.

in [4] for the convective Cahn-Hilliard model, order 2 in $\|\cdot\|_{L^2(\Omega)}$ and order 1 in $\|\cdot\|_{H^1(\Omega)}$ for the approximation of the variable $\Pi_1^h \phi$ have been approached. On the other hand, order around 2 in $\|\cdot\|_{L^2(\Omega)}$ has been obtained for the approximations of p and $\mathbf{u}$, the latter probably affected by the order of convergence in the approximation of $\Pi_1^h \phi$. Finally, order around 2 in $\|\cdot\|_{H^1(\Omega)}$ seems to have been achieved by the approximation of $\mathbf{u}$.

Remark 5.2. *Several works such as [12, 13, 18, 39] have carried out a careful error analysis of both coupled and decoupled finite element approximations of phase-field models coupled with fluid motion such as the CHNS system or related models. However, most of these works have focused on the case of constant or non-degenerate mobility and constant density and their results are based on the energy-stability property of the proposed approximations. It is left for a future work to study whether these techniques can be extended and applied to derive error estimates for our proposed coupled and decoupled approximations, (10) and (34), respectively.*

5.2 Mixing bubbles

For this test we keep the same initial conditions as in the previous test but with $\chi = 100$. Again, this initial condition can be seen in Figure 1.

In Figure 2 we have plotted the evolution in time of the approximation obtained using both the coupled and the decoupled schemes, (10) and (34), respectively, with $h \approx 1.41 \cdot 10^{-2}$ and $\Delta t = 10^{-3}$. On the other hand, in Figure 3 (left) we can observe how the bounds are preserved
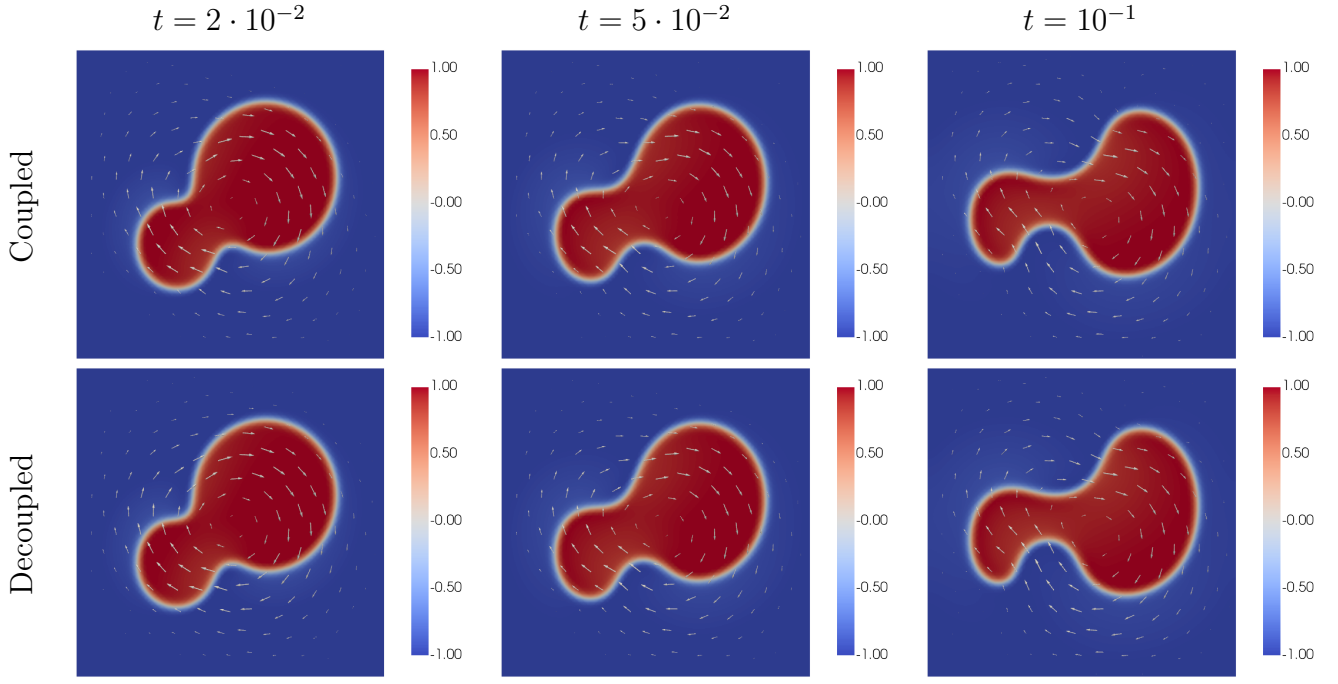
Figure 2: Evolution of $\Pi^h\phi$ over time in Test 5.2 ($\rho_1 = 1$, $\rho_2 = 100$).

as predicted by the previous analytical results. In addition, in Figure 3 (right) one may observe how the energy decreases both using the coupled approximation, as predicted by the theory above, and the decoupled approximation. In this case, the decoupled scheme is around 73% faster than the coupled scheme when run in series (using 8 threads to solve the linear systems) in the same computer.
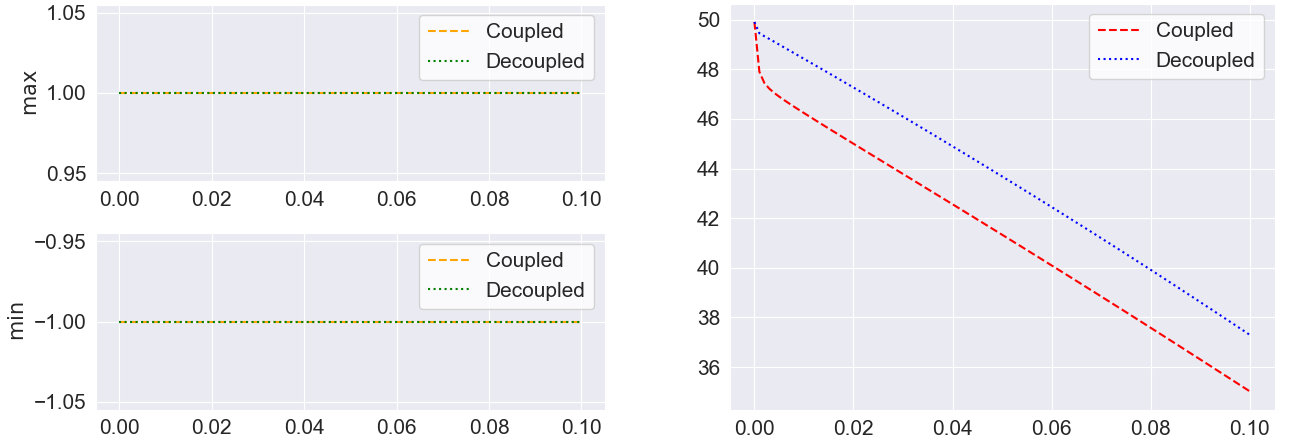

Figure 3: Left, maximum and minimum of $\Pi^h\phi$. Right, discrete energy. Test 5.2 ($\rho_1 = 1$, $\rho_2 = 100$).

We would like to highlight that even with this simple test one can find situations where the discrete energy of the decoupled scheme (34) increases exponentially while the approximation becomes completely unstable. In particular, in the case of two fluids with very different densities,

$$t = 4 \cdot 10^{-3} \qquad t = 5 \cdot 10^{-3} \qquad t = 6 \cdot 10^{-3}$$
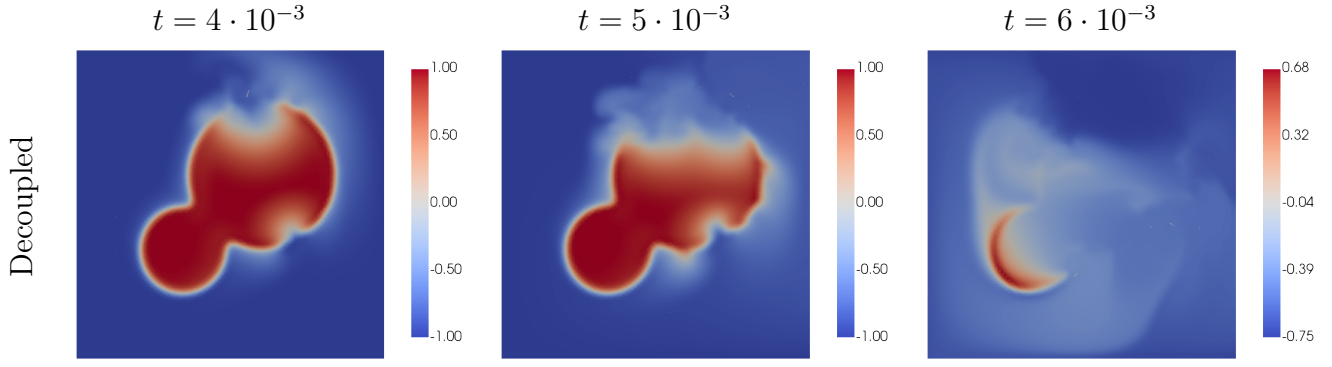
Figure 4: Evolution of $\Pi^h \phi$ over time in Test 5.2 ($\rho_1 = 1$, $\rho_2 = 1000$).
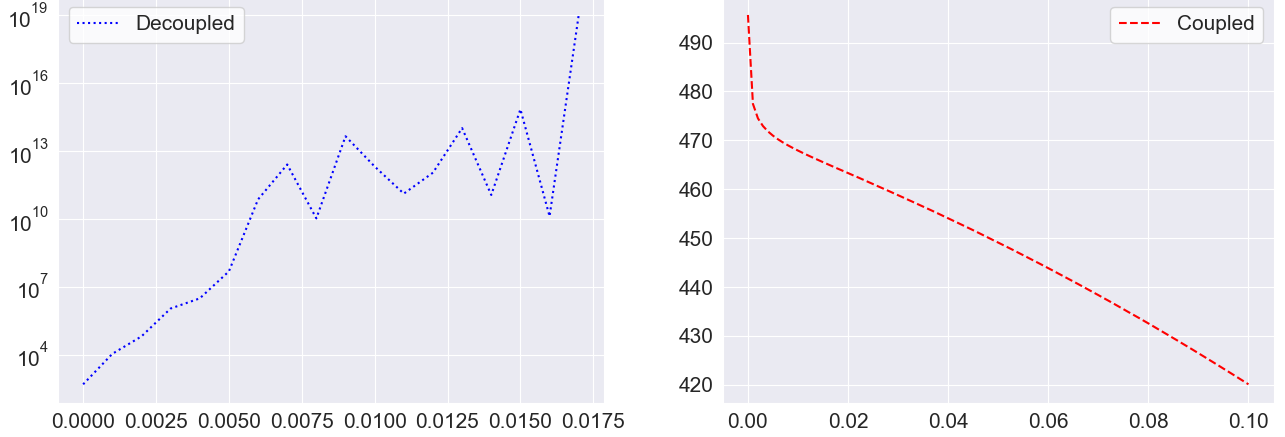
Figure 5: Left, discrete energy of the decoupled scheme. Right, discrete energy of the coupled scheme. Test 5.2 ($\rho_1 = 1$, $\rho_2 = 1000$).

for instance $\rho_1 = 1$ and $\rho_2 = 1000$, the approximation given by the decoupled scheme is totally nonphysical (see Figure 4) as its energy grows to infinity (see Figure 5, left) until the nonlinear solver is not able to converge to an approximation. Conversely, the energy stability property of the coupled scheme (10) makes it much more robust and, in this case, this approach is capable of providing a physical approximation where the energy does decrease over time as predicted by the theoretical results (see Figure 5, right). We omit the figures of the solution given by the coupled scheme as it is barely distinguishable from those shown in Figure 2.

5.3 A heavier bubble falling in a lighter medium

Now, we perform a test in which we define the following initial condition: $\mathbf{u}_0 = 0$ and

$$\phi_0(x, y) = \tanh\left(\frac{0.2 - \sqrt{x^2 + y^2}}{\sqrt{2}\varepsilon}\right),$$

a bubble of density $\rho_2 = 100$ in a lighter medium of density $\rho_1 = 1$, plotted in Figure 6. Moreover, we have added a term $-\rho(\phi)\boldsymbol{g}$ on the right-hand side of equation (1a) acting as the gravitational
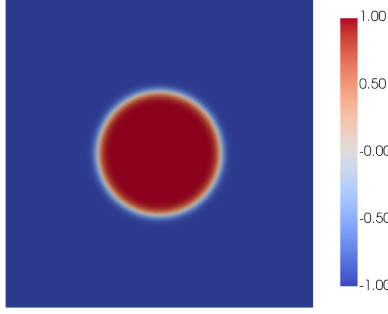
Figure 6: Initial condition of Test 5.3.

forces pushing the heavier bubble down to the bottom of the domain Ω. In our case, we have chosen $\boldsymbol{g} = (0, 1)$ and we have treated this term implicitly in (10) and explicitly in (34).
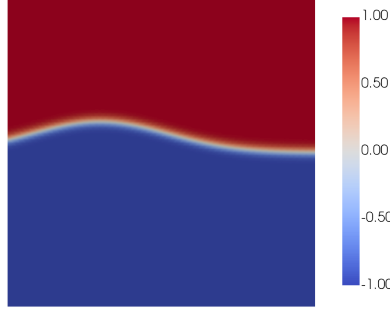
In this case, we have shown in Figure 8 the evolution in time of the solution using (10) and (34) with $h \approx 1.41 \cdot 10^{-2}$ and $\Delta t = 10^{-4}$. The result is qualitatively similar to the ones shown in previous studies such as [27]. Also, the bounds are preserved as shown in Figure 7 (left). In this case, the energy does not necessarily decrease due to the gravitational forces but, as one may observe in Figure 7 (right), the behavior of the energy is similar using both approaches.

We have noticed that the decoupled scheme is around 75% faster than the coupled approach in this test.
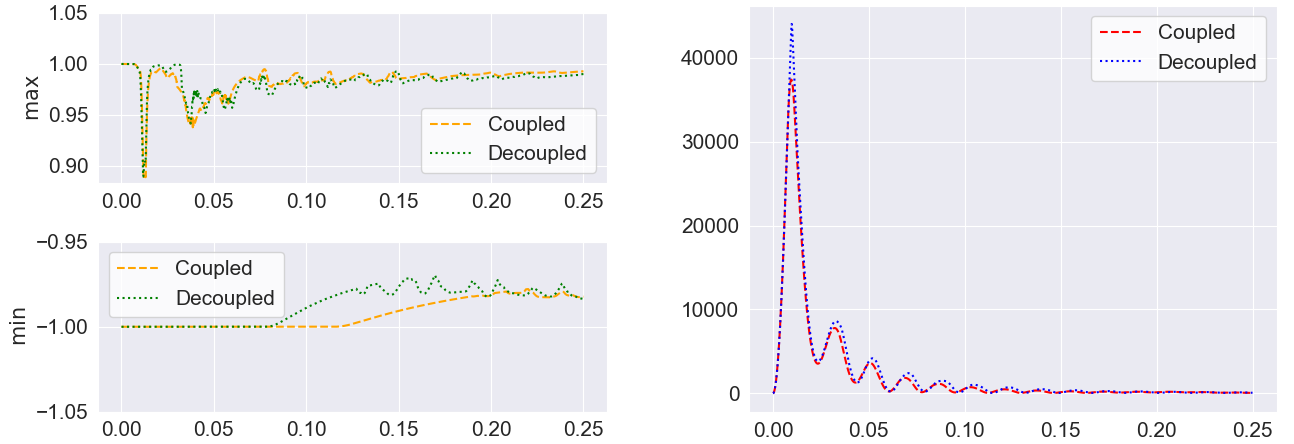
Figure 7: Left, maximum and minimum of $\Pi^h \phi$. Right, discrete energy. Test 5.3.
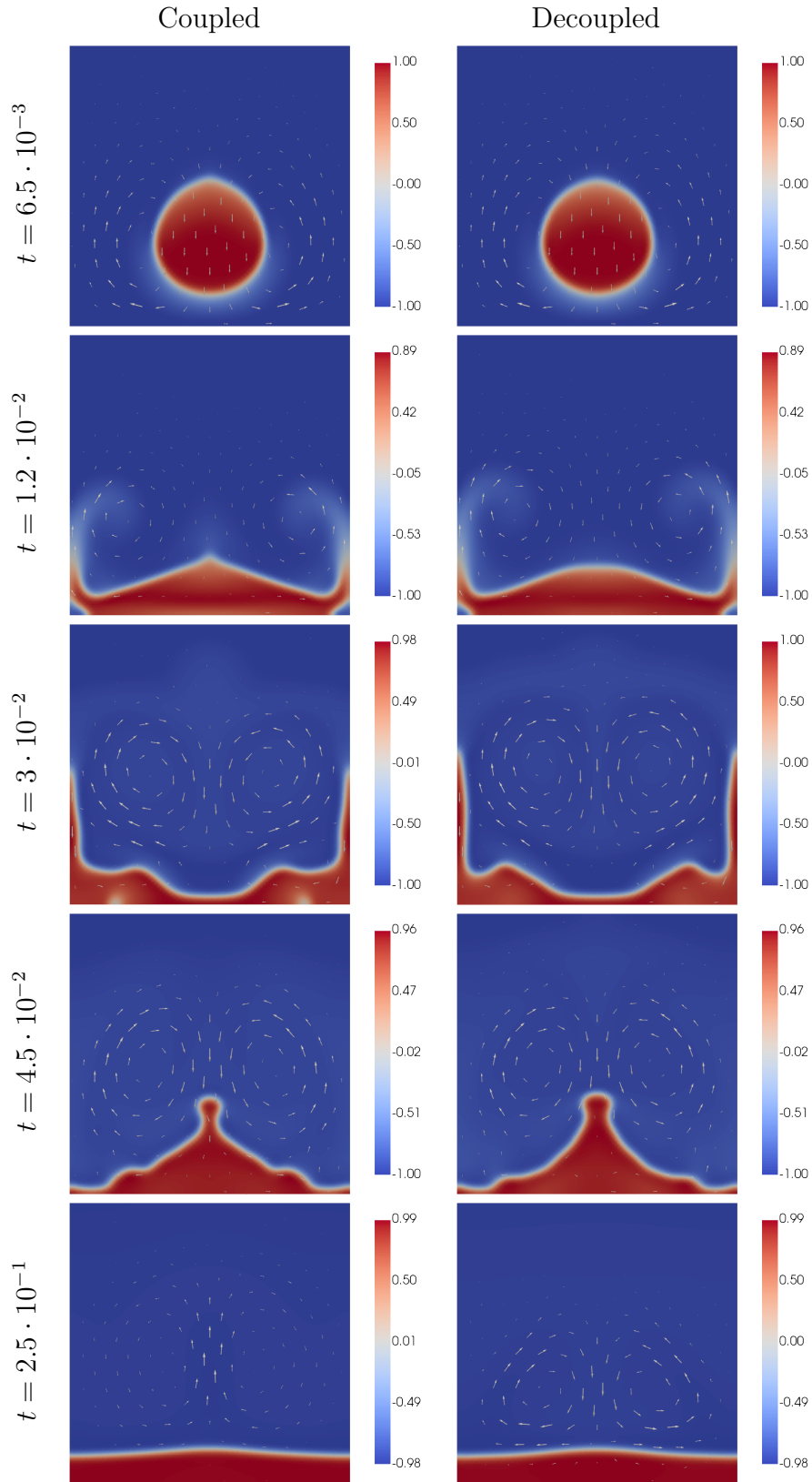
Figure 8: Evolution of $\Pi^h \phi$ over time in Test 5.3.

5.4   A Rayleigh-Taylor type instability

Finally, we carry out a benchmark Rayleigh-Taylor type instability test based on the one shown in [27] for which we define the following initial condition: $\mathbf{u}_0 = 0$ and

$$\phi_0(x, y) = \tanh\left(\frac{y - (0.1\exp(-(x+0.2)^2/0.1))}{\sqrt{2}\varepsilon}\right),$$

plotted in Figure 9. Again, we add the gravity term $-\rho(\phi)\boldsymbol{g}$ with $\boldsymbol{g} = (0, 1)$ in the RHS of equation (1a).

Figure 9: Initial condition of Test 5.4.

The evolution in time of the solution using (10) and (34) with $h \approx 1.41 \cdot 10^{-2}$ and $\Delta t = 10^{-4}$ can be seen in Figure 11. Again, despite the difficulty of this test due to the fast dynamics involved, the results are qualitatively similar to the ones shown in previous works such as [27]. In Figure 10 (left) we plot the evolution of the maximum and minimum of the regularized phase-field function, where we can observe that the bounds are indeed preserved as predicted by the theory. In addition, one may observe in Figure 10 (right), the behavior of the energy is similar using both approaches.

The decoupled scheme is around 39% faster than the coupled scheme in this test.
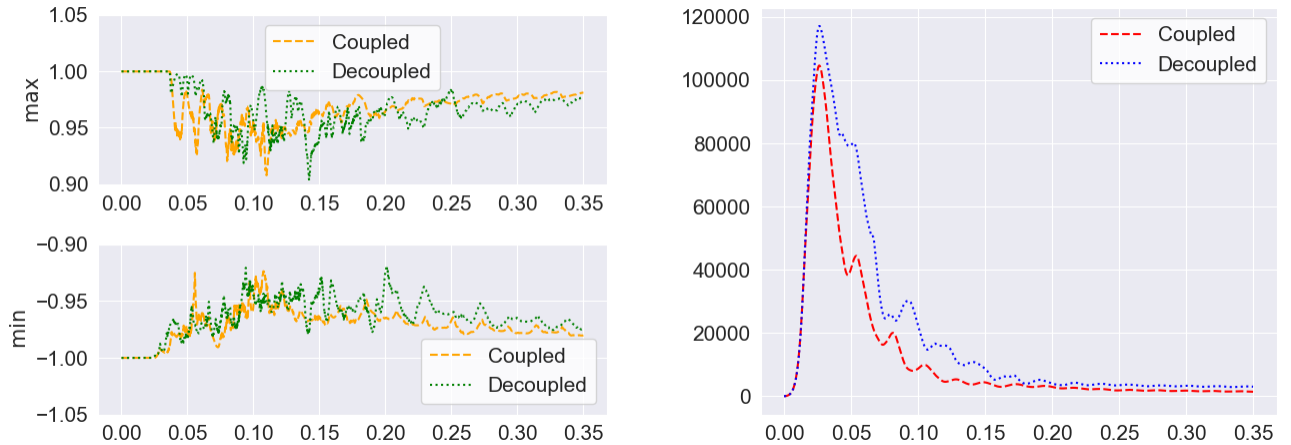
Figure 10: Left, maximum and minimum of $\Pi^h\phi$. Right, discrete energy. Test 5.4.
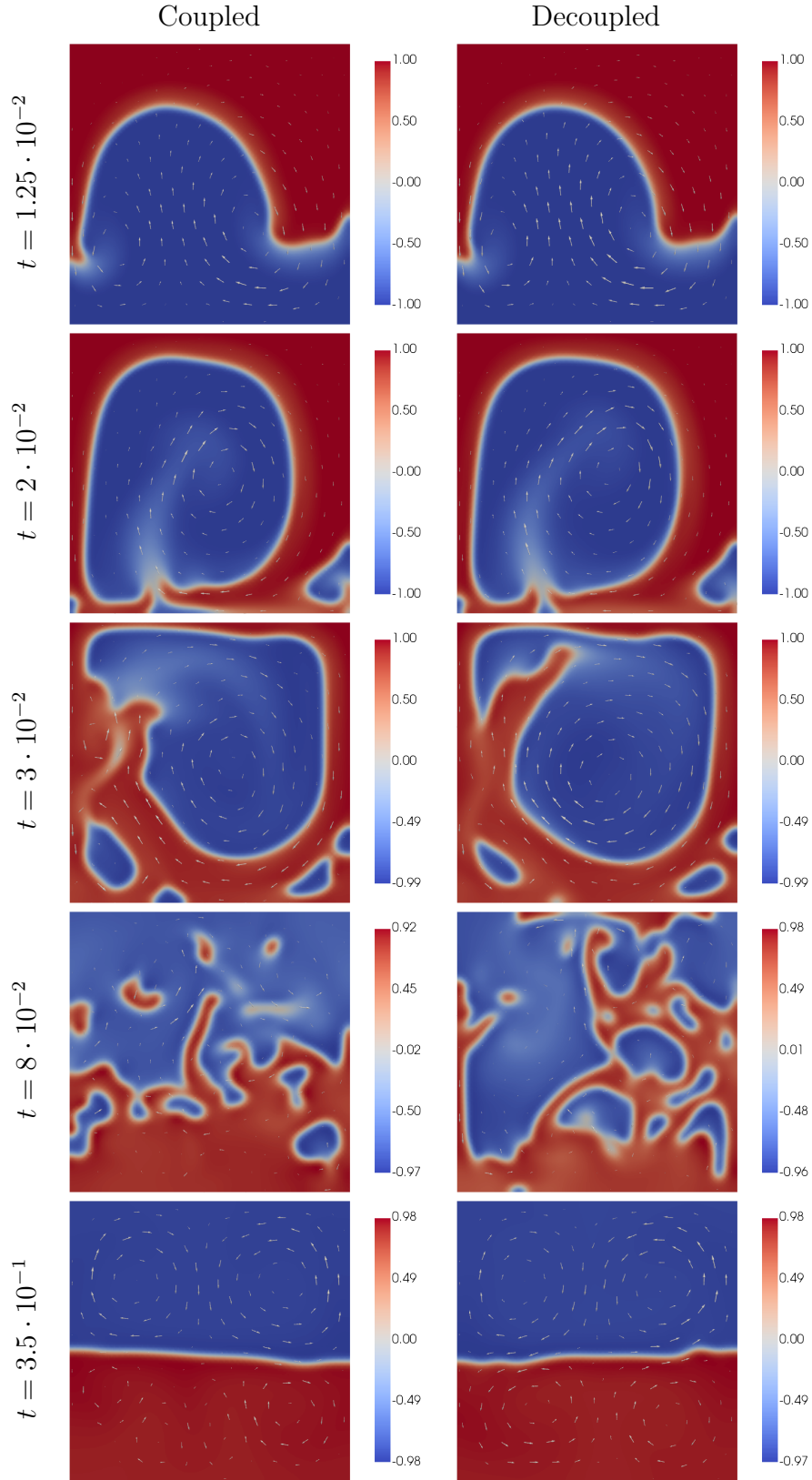
Figure 11: Evolution of $\Pi^h\phi$ over time in Test 5.4.

Acknowledgements

References

[1] H. Abels, H. Garcke, and G. Grün. Thermodynamically consistent, frame indifferent diffuse interface models for incompressible two-phase flows with different densities. *Mathematical Models and Methods in Applied Sciences*, 22(03):1150013, 2012. DOI: 10.1142/S0218202511500138.

[2] D. Acosta-Soba, F. Guillén-González, and J. R. Rodríguez-Galván. A structure-preserving upwind DG scheme for a degenerate phase-field tumor model. *Computers & Mathematics with Applications*, 152:317–333, 2023. DOI: 10.1016/j.camwa.2023.10.028.

[3] D. Acosta-Soba, F. Guillén-González, and J. R. Rodríguez-Galván. An Unconditionally Energy Stable and Positive Upwind DG Scheme for the Keller–Segel Model. *Journal of Scientific Computing*, 97(18), 2023. DOI: 10.1007/s10915-023-02320-4.

[4] D. Acosta-Soba, F. Guillén-González, and J. R. Rodríguez-Galván. An upwind DG scheme preserving the maximum principle for the convective Cahn–Hilliard model. *Numerical Algorithms*, 92(3):1589–1619, 2023. DOI: 10.1007/s11075-022-01355-2.

[5] M. S. Alnaes, A. Logg, K. B. Ølgaard, M. E. Rognes, and G. N. Wells. Unified Form Language: A domain-specific language for weak formulations of partial differential equations. *ACM Transactions on Mathematical Software*, 40, 2014. DOI: 10.1145/2566630.

[6] P. R. Amestoy, I. S. Duff, J.-Y. L'Excellent, and J. Koster. A fully asynchronous multifrontal solver using distributed dynamic scheduling. *SIAM Journal on Matrix Analysis and Applications*, 23(1):15–41, 2001. DOI: 10.1137/S0895479899358194.

[7] P. R. Amestoy, A. Guermouche, J.-Y. L'Excellent, and S. Pralet. Hybrid scheduling for the parallel solution of linear systems. *Parallel computing*, 32(2):136–156, 2006. DOI: 10.1016/j.parco.2005.07.004.

[8] S. Balay, S. Abhyankar, M. F. Adams, S. Benson, J. Brown, P. Brune, K. Buschelman, E. Constantinescu, L. Dalcin, A. Dener, V. Eijkhout, J. Faibussowitsch, W. D. Gropp, V. Hapla, T. Isaac, P. Jolivet, D. Karpeev, D. Kaushik, M. G. Knepley, F. Kong, S. Kruger, D. A. May, L. C. McInnes, R. T. Mills, L. Mitchell, T. Munson, J. E. Roman, K. Rupp, P. Sanan, J. Sarich, B. F. Smith, S. Zampini, H. Zhang, H. Zhang, and J. Zhang. PETSc/TAO Users Manual. Technical report ANL-21/39 - Revision 3.19, Argonne National Laboratory, 2023. DOI: 10.2172/1968587.

[9] D. Boffi, F. Brezzi, and M. Fortin. *Mixed finite element methods and applications*, volume 44. Springer, 2013. DOI: 10.1007/978-3-642-36519-5.

[10] F. Boyer. A theoretical and numerical model for the study of incompressible mixture flows. *Computers & fluids*, 31(1):41–68, 2002. DOI: 10.1016/s0045-7930(00)00031-1.

[11] W. Chen, J. Jing, C. Wang, and X. Wang. A positivity preserving, energy stable finite difference scheme for the Flory–Huggins–Cahn–Hilliard–Navier-Stokes system. *Journal of Scientific Computing*, 92(31), 2022. DOI: 10.1007/s10915-022-01872-1.

[12] W. Chen, S. Wang, Y. Zhang, D. Han, C. Wang, and X. Wang. Error estimate of a decoupled numerical scheme for the Cahn–Hilliard–Stokes–Darcy system. *IMA Journal of Numerical Analysis*, 42(3):2621–2655, 2022. DOI: 10.1093/imanum/drab046.

[13] Y. Chen, Y. Huang, and N. Yi. Error analysis of a decoupled, linear and stable finite element method for Cahn–Hilliard–Navier–Stokes equations. *Applied Mathematics and Computation*, 421:126928, 2022. DOI: 10.1016/j.amc.2022.126928.

[14] P. G. Ciarlet. *The finite element method for elliptic problems*. SIAM, 2002. DOI: 10.1137/1.9780898719208.

[15] F. H. Clarke. *Optimization and nonsmooth analysis*. SIAM, 1990. DOI: 10.1137/1.9781611971309.

[16] L. D. Dalcin, R. R. Paz, P. A. Kler, and A. Cosimo. Parallel distributed computing using python. *Advances in Water Resources*, 34(9):1124 –1139, 2011. DOI: 10.1016/j.advwatres.2011.04.013. New Computational Methods and Software Tools.

[17] D. A. Di Pietro and A. Ern. *Mathematical Aspects of Discontinuous Galerkin Methods*, volume 69 of *Mathématiques et Applications*. Springer, 2012. DOI: 10.1007/978-3-642-22980-0.

[18] A. E. Diegel, C. Wang, X. Wang, and S. M. Wise. Convergence analysis and error estimates for a second order accurate finite element method for the Cahn–Hilliard–Navier–Stokes system. *Numerische Mathematik*, 137:495–534, 2017. DOI: 10.1007/s00211-017-0887-5.

[19] H. Ding, P. D. M. Spelt, and C. Shu. Diffuse interface model for incompressible two-phase flows with large density ratios. *Journal of Computational Physics*, 226(2):2078–2095, 2007. DOI: 10.1016/j.jcp.2007.06.028.

[20] A. Ern and J. L. Guermond. *Theory and practice of finite elements*, number 159 in Applied mathematical sciences. Springer, 2010. DOI: 10.1007/978-1-4757-4355-5.

[21] D. J. Eyre. An unconditionally stable one-step scheme for gradient systems. *Unpublished article*, 1997. https://citeseerx.ist.psu.edu/document?repid=rep1&type=pdf&doi=4f016a98fe25bfc06b9bcab3d85eeaa47d3ad3ca.

[22] F. Frank, C. Liu, F. O. Alpak, and B. Rivière. A finite volume/discontinuous Galerkin method for the advective Cahn–Hilliard equation with degenerate mobility on porous domains stemming from micro-CT imaging. *Computational Geosciences*, 22:543–563, 2018. DOI: 10.1007/s10596-017-9709-1.

[23] G. Grün, F. Guillén-González, and S. Metzger. On fully decoupled, convergent schemes for diffuse interface models for two-phase flow with general mass densities. *Communications in Computational Physics*, 19(5):1473–1502, 2016. DOI: 10.4208/cicp.scpde14.39s.

[24] J. L. Guermond, P. Minev, and J. Shen. An overview of projection methods for incompressible flows. en. *Computer Methods in Applied Mechanics and Engineering*, 195(44-47):6011–6045, 2006. DOI: 10.1016/j.cma.2005.10.010.

[25] J. L. Guermond and J. Shen. A new class of truly consistent splitting schemes for incompressible flows. *Journal of computational physics*, 192(1):262–276, 2003. DOI: 10.1016/j.jcp.2003.07.009.

[26] F. Guillén-González and G. Tierra. On linear schemes for a Cahn–Hilliard diffuse interface model. *Journal of Computational Physics*, 234:140–171, 2013. DOI: 10.1016/j.jcp.2012.09.020.

[27] F. Guillén-González and G. Tierra. Splitting Schemes for a Navier-Stokes-Cahn-Hilliard Model for Two Fluids with Different Densities. *Journal of Computational Mathematics*, 32(6):643–664, 2014. DOI: 10.4208/jcm.1405-m4410.

[28] M. E. Gurtin, D. Polignone, and J. Vinals. Two-phase binary fluids and immiscible fluids described by an order parameter. *Mathematical Models and Methods in Applied Sciences*, 6(06):815–831, 1996. DOI: 10.1142/S0218202596000341.

[29] P. C. Hohenberg and B. I. Halperin. Theory of dynamic critical phenomena. *Reviews of Modern Physics*, 49(3):435, 1977. DOI: 10.1103/RevModPhys.49.435.

[30] J. Kim. Phase-field models for multi-component fluid flows. *Communications in Computational Physics*, 12(3):613–661, 2012. DOI: 10.4208/cicp.301110.040811a.

[31] C. Liu, D. Ray, C. Thiele, L. Lin, and B. Rivière. A pressure-correction and bound-preserving discretization of the phase-field method for variable density two-phase flows. *Journal of Computational Physics*, 449:110769, 2022. DOI: 10.1016/j.jcp.2021.110769.

[32] C. Liu, B. Rivière, J. Shen, and X. Zhang. A simple and efficient convex optimization based bound-preserving high order accurate limiter for Cahn–Hilliard–Navier–Stokes system. *arXiv preprint*, 2023. DOI: 10.48550/arXiv.2307.09726.

[33] J. Lowengrub and L. Truskinovsky. Quasi–incompressible Cahn–Hilliard fluids and topological transitions. *Proceedings of the Royal Society of London. Series A: Mathematical, Physical and Engineering Sciences*, 454(1978):2617–2654, 1998. DOI: 10.1098/rspa.1998.0273.

[34] B. Rivière. *Discontinuous Galerkin Methods for Solving Elliptic and Parabolic Equations: Theory and Implementation*. SIAM, 2008. DOI: 10.1137/1.9780898717440.

[35] M. W. Scroggs, I. A. Baratta, C. N. Richardson, and G. N. Wells. Basix: a runtime finite element basis evaluation library. *Journal of Open Source Software*, 7(73):3982, 2022. DOI: 10.21105/joss.03982.

[36] M. W. Scroggs, J. S. Dokken, C. N. Richardson, and G. N. Wells. Construction of Arbitrary Order Finite Element Degree-of-Freedom Maps on Polygonal and Polyhedral Cell Meshes. *ACM Transactions on Mathematical Software*, 48(2), 2022. DOI: 10.1145/3524456.

[37] J. Shen, J. Xu, and J. Yang. The scalar auxiliary variable (SAV) approach for gradient flows. *Journal of Computational Physics*, 353:407–416, 2018. DOI: 10.1016/j.jcp.2017.10.021.

[38] J. Shen and X. Yang. Decoupled, energy stable schemes for phase-field models of two-phase incompressible flows. *SIAM Journal on Numerical Analysis*, 53(1):279–296, 2015. DOI: 10.1137/140971154.

[39] V. Styles, D. Kay, and R. Welford. Finite element approximation of a Cahn–Hilliard–Navier–Stokes system. *Interfaces and free Boundaries*, 10(1):15–43, 2008. DOI: 10.4171/IFB/178.

[40] C. B. Sullivan and A. Kaszynski. PyVista: 3D plotting and mesh analysis through a streamlined interface for the Visualization Toolkit (VTK). *Journal of Open Source Software*, 4(37):1450, 2019. DOI: 10.21105/joss.01450.

[41] M. F. P. Ten Eikelder, K. G. Van Der Zee, I. Akkerman, and D. Schillinger. A unified framework for Navier–Stokes Cahn–Hilliard models with non-matching densities. *Mathematical Models and Methods in Applied Sciences*, 33(01):175–221, 2023. DOI: 10.1142/S0218202523500069.

[42] J. D. van der Waals. The thermodynamic theory of capillarity flow under the hypothesis of a continuous variation of density. *Verhandel. Konink. Akad. Weten. Amsterdam*, 1(8), 1879. DOI: 10.1007/BF01011513. Translated version (original in Dutch).